Task 1. Iron Catalyst Preparation

The objective of this task is to produce robust intermediate- and high-α catalysts.

A. Fischer-Tropsch Synthesis: Activity and Selectivity for Group I Alkali Promoted Iron-Based Catalysts

Abstract

The impact of the Group I alkali metals upon the activity of iron catalysts has been obtained at medium pressure synthesis conditions and at the same conversion levels. The relative impact of the alkali metal depends upon the conversion level with potassium being the promoter that impacts the highest activity at all conversion levels. At low conversions, Li is nearly as effective as potassium in improving the catalytic activity but is the poorest promoter at high conversion levels. In fact, three alkalis (Li, Cs and Rb) should be viewed as inhibitors since they decrease the catalytic activity for CO conversion below that of the unpromoted iron catalyst. The differences in the impact of the various Group I alkali metals at lower (<~40%) conversions are slight but become much greater at higher CO conversion levels. The major differences of the alkali metals at higher conversion levels is due to the impact of the promoter upon the water-gas-shift reaction. At higher conversion levels, with a syngas of $H_2/CO = 0.7$, the water-gas-shift reaction becomes rate controlling because hydrogen production becomes the rate limiting factor in the Fischer-Tropsch synthesis. The basicity of the promoter appears to be the determining factor for the rate of catalyst deactivation and on the secondary hydrogenation of ethene.

Keywords: promoter, alkali; Fischer-Tropsch synthesis, iron catalyst; Group I metal; potassium, lithium, cesium, rubidium

Introduction

The Fischer-Tropsch synthesis (FTS) offers the possibility of converting a mixture of hydrogen and carbon monoxide (synthesis gas or "syngas") into clean hydrocarbons, free from sulfur. This syngas is usually produced from natural gas or coal, and exhibits a lower H_2/CO ratio for coal gasification. As carbon number of the hydrocarbon produced can range from 1 to over 100, this process can be used to produce high-value transportation fuels, such as gasoline (C_5-C_{11}) and diesel fuels (C_{12}-C_{18}). Several metals, such as nickel, cobalt, ruthenium and iron, have been shown to be active for this reaction (1), which can be represented as:

$$CO + \left(1 + \frac{n}{2}\right) H_2 \rightarrow CH_n + H_2O \qquad \textbf{(1)}$$

where n is the average H/C ratio, usually between 2.1 and 2.5

However, only iron- and cobalt-based catalysts appear to be economically feasible at an industrial scale. Because catalysts may also be active for the water-gas shift (WGS) reaction

$$CO + H_2O \rightarrow CO_2 + H_2, \qquad \textbf{(2)}$$

a syngas presenting a low H_2/CO ratio, as that produced by coal gasification in advanced gasifiers, can be directly used for FTS. Further, this reaction consumes the water product, which may act as a poison for FTS catalysts, as the following expression for the Fischer-Tropsch rate shows (2):

$$-r_{CO+H_2} = \frac{kP_{H_2}}{1 + b(P_{H_2O}/P_{H_2}P_{CO})} \qquad \textbf{(3)}$$

Typical iron-based catalysts contain varying amounts of structural addatives, such as silica or alumina, and chemical promoters, such as potassium and copper, known to, for example, increase the overall FTS activity or to facilitate the reduction of iron oxide to metallic iron during hydrogen activations (3). Many studies have been made on potassium-promoted

catalysts, which have been shown to either decrease or increase the FTS activity (1) of an iron catalyst. However, few reports of the effect of the other alkalis are available (4). One report shows that their effectiveness decreases in the order Rb, K, Na, Li (1). While much work has been conducted, there are few studies that provide data that allow a direct comparison of the effectiveness of the various Group I alkali metals. One example of a direct comparison utilized atmospheric pressure reaction conditions and an iron catalyst base that was prepared by the ignition of the nitrate salt. The conversion with these catalysts, presumably having low activity, was not stable with time (Figure 1) (4,5) and showed that K and Rb were the superior alkali promoters. Dry (6) reported for precipitated iron catalysts that the stronger bases of Group I elements are key promoters and that the relative activities of catalysts containing equal atomic amounts of Group I metals were: K, 100; Na and Rb ≈ 90; Li, ~ 40. Dry indicated that Rb was out of line, probably due to its high wax selectivity. Dry and Oosthuizen (7) utilized fused iron catalysts in which the alkali was present during the fusion step or was added by impregnation after the fusion step. For the reduced catalyst, the basicity, determined from CO_2 adsorption, increased in the order Ba, Li, Ca, Na and K. The amount of methane decreased as the surface basicity increased. The activity data were obtained at atmospheric pressure at 290°C with a gas having a H_2/CO ratio of 3.2. Pilot plant data were obtained at 250 psig (1.72 MPa) and 593 K, in a fluidized bed reactor, and these supported the trend observed at one atmosphere pressure.

Röper (8) provides a ranking of the efficiency of alkali promoters as: Rb 〉 K 〉 Na 〉 Li. However, this ranking was based at least in part on the results described above.

In spite of the recognized importance of the alkali promoter, data to document their relative influence are not abundant. Furthermore, the data that are available have been obtained under conditions that may not be applicable for slurry phase operations. The purpose of this study is to compare the effects of iron-based catalysts, promoted with different alkalis (Li, Na, K,

Rb and Cs) on FTS. The catalysts have been used in a slurry reactor and data were obtained over a wide range of syngas space-velocities. Further, activities and selectivities, as well as hydrocarbon production rates and compositions, have been obtained at similar carbon monoxide conversions.

Experimental

Catalysts

A precipitated iron-silica catalyst with atomic ratio 100Fe/4.6Si was prepared by continuous coprecipitation in a stirred tank reactor, using a process which has been described previously (9). The alkali (Li, Na, K, Rb and Cs) was then added by incipient wetness impregnation with an aqueous alkali carbonate to obtain an alkali:iron atomic ratio of 1.44:100. Copper, a known promoter, was not added in order to avoid complications from its presence. The catalyst, promoted or unpromoted, undergoes complex physical and chemical changes during activation and use (10). The physical changes for unpromoted and potassium promoted iron show that the surface area of the catalyst increases slowly with use, presumably due to the slow deposition of high surface area carbon (10). The pore size distribution changes to eliminate the microporosity during the activation step and during use the average pore size of the mesoporosity increases slowly (10).

Reaction System and Product Analysis

A 1-liter continuous stirred tank reactor (CSTR) was used. Analysis of all products were made using a variety of chromatographs. More details of the reaction system and the product analysis have been reported previously (11).

The catalyst (5 g) was mixed in the reactor with 310 g of melted octacosane, previously treated to remove a bromide impurity, that was used as the start-up solvent. The stirring speed was set at 750 rpm before the reactor pressure was increased to 175 psig (1.308 MPa) with

carbon monoxide at a flow rate of 25 NL/hr. The reactor temperature was then increased to 543 K at a heating rate of 2 K/min. The catalyst was pretreated at 543 K for a total of 22 hours.

After this period, the reactor was fed with syngas at a constant H_2/CO ratio of 0.67 by introducing and increasing the H_2 flow during a 2 hr period. The pressure, temperature and stirring speed were maintained at 175 psig (1.308 MPA), 543 K and 750 rpm, respectively. After the catalyst reached steady state, as evidenced by a constant syngas conversion, the feed gas space velocity was varied between 5 and 65 NL/hr/g(Fe) and maintained at each flow rate for 24 hours. The catalyst activity was measured periodically at preset "standard" conditions (a space velocity of 10 N/hr/g(Fe)) to determine whether the catalyst had deactivated. Conversion versus reaction time was plotted for the "standard" conditions and this relationship was used to correct each measured activity to that of the fresh catalyst. The conversions of carbon monoxide, the exit flow rate being known, was measured. FTS products were collected in three traps maintained at 473, 373 and 273 K (11), and then weighed and analyzed.

Results

Carbon Monoxide Conversion

The conversion values are corrected, according to the linear deactivation rate obtained from the values of conversions at different times-on-stream, by returning to the standard flow rate of 10NL/hr/g(Fe) at intervals during the run (Figure 2). The lowest deactivation rate is obtained by the lithium promoted catalyst, with a rate of 0.48% CO conversion/week. The deactivation rates of sodium, potassium, rubidium and cesium catalysts are 0.84, 1.23, 1.80 and 2.75% CO conversion/day, respectively. We can thus conclude that the more basic the alkali, the higher the deactivation rate.

The experimental CO conversion data cover a wide range of values, from about 15 to over 90%. Conversions are dependent on space-time and alkali. The potassium promoted

catalyst shows the highest conversions, especially at higher space-times. The activity rankings are obtained at 20 through 60% CO conversion levels by comparing the relative flow rates needed to obtain this conversion level. At the higher flow rates, the catalyst promoted with lithium exhibits the same conversion as the catalyst that contains potassium, but above a space-time of about 0.1 hr g(Fe)/NL the Li-promoted catalyst exhibits the lowest conversions. At 20% CO conversion level, the unpromoted catalyst yielded the same activity as K, Na and Li promoted catalysts; however, for this conversion level the Cs and Rb promoted catalyst is only about half as active as the K-promoted catalyst. At the 40% conversion level, the ranking changes somewhat. The K- and Na-promoted catalysts have about the same activity, but the unpromoted catalyst now has only about 0.68 of the activity of the K-promoted catalyst. At this CO conversion level, Li, Rb and Cs promoted catalysts exhibit only about half the activity of the K-promoted catalyst (Table 1). At the 60% CO conversion level, the Na-promoted and the unpromoted catalyst has only about 0.64 of the activity of the K-promoted catalyst. The Rb-promoted catalyst shows only about 0.33 the activity of the K-promoted catalyst and the Cs- and Li-promoted catalyst have only 0.28 the activity of the K-promoted catalyst.

Product Partial Pressures

Since a CSTR was used, the partial pressures are the same throughout the reactor. A first appreciation of the WGS reaction activity can be made from plots of water (Figure 3) and carbon dioxide (Figure 4) partial pressures in the reactor. For all catalysts, the water partial pressure shows a rapid increase at low space times, then reaches a maximum before declining. This result is consistent with previous studies made with potassium promoted iron catalysts (12). The catalyst promoted with lithium shows the highest water partial pressure at all space-times. The initial increase, at CO conversions close to that of potassium, indicates that this catalyst is less active for the WGS reaction than the other alkali metal promoted catalyst. This can also be

verified by considering the carbon dioxide partial pressure, which is much higher for the catalyst promoted with potassium.

Rates of FTS and WGS Reaction

As mentioned earlier, carbon monoxide can be converted either into hydrocarbon products and water, or into carbon dioxide and hydrogen. It is thus interesting to compare the rates of these two reactions and they can be calculated:

$$r_{WGS} = r_{CO_2} \quad \textbf{(4)}$$

and

$$r_{FTS} = r_{CO} - r_{CO_2} \quad \textbf{(5)}$$

As the WGS reaction needs the water produced by the FTS, an inequality:

$$r_{WGS} \leq r_{FTS} \quad \textbf{(6)}$$

is always observed. All FTS rates exhibit dependence on space-time and decrease with increasing space-time (Figure 5). Further, all WGS-reaction rates show a maximum at about the same space-time (Figure 6), and this occurs at about the same time as when the water partial pressure attains its maximum value.

The K-promoted catalyst exhibits the highest WGS rates over the total flow range utilized. The Na promoted catalyst is almost as active at the K-promoted catalyst. Surprisingly, the unpromoted iron catalyst has a higher rate than three of the alkali promoted catalysts, and since it does not appear that the maximum rate was attained at even the highest flow used, the iron catalytic activity may be as high as any of the alkali promoted catalysts. At the intermediate flow rates, the Li-promoted catalyst is more active than the Cs- and Rb-promoted catalysts but these three promoted catalysts approach a similar rate at about space velocity of about 0.1.

Carbon Utilization

A perceived disadvantage of using iron-based catalysts is that a large proportion of the carbon monoxide that is converted into carbon dioxide rather than the desired hydrocarbons. This is a perceived disadvantage since the rejection of carbon dioxide results in a lower conversion of hydrogen. The extent of the WGS reaction needs to be defined. One measure is the WGS-reaction quotient, which can be expressed as:

$$RQ_{WGS} = \frac{P_{CO_2} P_{H_2}}{P_{CO} P_{H_2O}} \quad \textbf{(7)}$$

However, at lower conversion levels RQ_{WGS} may be dominated by the large partial pressures of the unconverted hydrogen and carbon monoxide. It is illustrative to consider the extent of the WGS-reaction by calculating the fraction of carbon monoxide converted to hydrocarbons:

$$Fraction\ of\ \ CO\ producing\ hydrocarbon = \frac{r_{FTS}}{r_{CO}} \quad \textbf{(8)}$$

As the rate of the FTS is always at least as large as the WGS reaction rate, the fraction is always greater than 0.5. It is immediately evident that the fractions of CO converted to hydrocarbons, and therefore the ratio of the relative rates for FTS and WGS, drop dramatically with space-time (Figure 7). The catalyst promoted with potassium shows the lowest fraction of carbon monoxide transformed into hydrocarbon products at almost all space-times. However, the fractions for all catalysts approach a constant value at the high space-times Even so, at high space-times, the Cs-promoted catalyst make slightly more efficient utilization of the carbon monoxide to produce hydrocarbon products.

Hydrocarbon Product Selectivity

FTS produces many hydrocarbons and it is impossible to produce only a desired product, such as gasoline (C_5-C_{11}) or diesel fuels (C_{12}-C_{18}). Figure 8 shows the hydrocarbon product distributions over different alkali metal promoted iron catalysts at a space velocity of 10 NL/hr/g-Fe. Alkalinity did not affect the C_1 production while it yielded a 5-7% difference in other fractions. The umpromoted catalyst produced the highest C_2-C_4 and the lowest gasoline (C_5-C_{11}) and diesel (C_{12}-C_{18}) fractions. Among the Group I alkalis, Na yielded the highest C_2-C_4 and gasoline fractions and the lowest diesel and C_{19+} fractions. Potassium, however, produced the lowest C_2-C_4 and gasoline, but the highest C_{19+} fractions. Similar results were obtained from Li, Cs and Rd-promoted catalysts.

Another important selectivity is the fraction of the hydrocarbons that are represented by light hydrocarbon gases, especially methane. As shown in Figure 9, the fraction of methane produced does not increase rapidly over the CO conversion range of 20 to 90%. Except for the Li-promoted and the unpromoted iron catalysts, the fraction of methane in the hydrocarbon products does not depend upon the alkali promoter.

The fraction of alkenes can depend upon the amount of promoter and the data in Figure 10 clearly show that the fraction of ethene depends strongly upon the promoter. For the unpromoted catalyst, only about 20% of the C_2 hydrocarbons is represented by ethene. The Li- and Na-promoted catalysts produce about 50% of the unsaturated C_2 product, ethene. Cs-, Rb- and K-promoted catalysts have the highest olefin selectivity, producing about 80% of the unsaturated product, ethene. The fraction of alkene decreases as the CO conversion increases.

Discussion

The results obtained during this study for the promoted catalysts are directly comparable since the conversions were: (a) obtained under the same reaction conditions, (b) a common precipitated iron base catalyst was used and (c) the catalysts had the same atomic alkali content.

The relative catalytic activities for the alkali promoted catalysts are dependent upon the conversion levels as shown in Table 1. Thus, at low conversion levels, Li is about as effective as K but at intermediate and high conversion levels it is the least effective promoter. The WGS reaction is slower than the FT reaction so that it appears that the relative rates of the FT and WGS reactions is responsible for the difference in total CO conversion.

While the total conversion is an important consideration, in at least some instances the relative rates of FTS and WGS are more important; that is, selectivity is more important than productivity. The data in Figure 6 show that, at lower conversion levels, FTS is relatively rapid compared to WGS so that a higher fraction of CO is converted to hydrocarbons. The advantage of the more rapid FTS rate cannot be maintained throughout the CO conversion since the decreasing H_2/CO ratio causes the rate determining step to change from FTS to the WGS reaction. Thus, above about 50% CO conversion, the rate of FTS depends upon the production of hydrogen by the WGS reaction. It has been observed that the rate of FTS is not inhibited by the addition of water with the syngas feed, at least up to a ratio of $H_2O/CO = 0.3$; the only impact of the added water is to increase the rate of the WGS reaction (15). Thus, it does not appear that water partial pressure has a significant impact upon the FTS kinetics due to its impact by competitive adsorption, at least at the lower CO conversion levels.

The ranking of the effectiveness of the alkali metal promoters cannot be due only to their basicity unless the alkalis undergo changes in basicity in a way that depends upon CO conversion. While the amount of water that is present in the reactor may impact the basicity, it

does not appear that the differences in water partial pressure is large enough to make this a reasonable explanation. It appears more likely that the kinetic impact of water is responsible for the changes in the effectiveness of the promoters and its dependance on the CO conversion level. There appears to be two ways in which water may impact the relative effectiveness of the alkali promoters. First, at the lower conversion levels, water can impact the rate because of the competition of its adsorption with that of the CO and/or H_2 reactants and the nature of the alkali promoter may impact this factor differently. At the higher CO conversion levels, the depletion of hydrogen because of the slowness of the WGS reaction may become the more important factor. Thus, the least effective WGS catalyst will cause hydrogen depletion at a lower CO conversion level and force the FTS rate to be limited by the rate of the WGS reaction. As indicated above, the presence of added water did not impact the FTS rate at lower CO conversion levels to a measurable extent with the K-promoted catalyst and it is concluded that the impact of water does not impact the kinetics with the iron catalyst under low temperature conditions.

Basicity is a frequently used term in the literature and, together with acidity, forms the basis for much of catalysis. These terms are fundamental but the so-called acid-base "theories" are in reality merely definitions of what an acid or base is. Furthermore, apart from aqueous solutions and the well-established pH scale, the definitions are not quantitative. Nevertheless, it is convenient to use the terminology to describe catalysis. One area where this has been done is to describe promotion of iron catalysts (7).

The Lux-Flood definition describes acid-base chemistry in terms of the oxide ion. A base is an oxide donor and an acid is an oxide acceptor. This acidity scale may be based on the difference in the acidity parameters, $(a_B - a_A)$, of a metal oxide and a nonmetal oxide being the square root of the enthalpy of reaction of the acid and base (16). On this basis, with water

chosen to calibrate the scale at a value of 0.0, cesium oxide is the most basic oxide. The Group I oxides of interest have the following acidity (opposite to basicity) parameters: Cs_2O, -15.2; Rb_2O, -15.0; K_2O, -14.6; Na_2O, -12.5; and Li_2O, -9.2.

A complicating factor is the leveling effect. All acids and bases stronger than the characteristic cation and anion of the solvent will be "leveled" to the latter. Thus, in water solvent an acid will not be stronger than H_3O^+ and a base cannot be stronger than OH^-. In the Lux-Flood system, a base cannot be stronger than O^{2-}.

For Group I cations with a noble-gas configuration, in an aqueous solution, hydrolysis of the metal ion is greatest for Li. K^+, Rb^+ and Cs^+ are not measurably hydrolyzed in aqueous solution (17). Thus, based on an aqueous solution, the larger Group I metal cations are not basic. Considering the aqueous bases, the interaction between the metal ion and the hydroxide ion is essentially electrostatic so that pK_b varies in a linear fashion with q^2/r, where q is the charge on the ion and r is the ionic radius and pK_b refers to the loss of the hydroxide group. On this basis, LiOH (pK_b = 0.18) has the lowest basicity of the alkali metals. NaOH (pK_b = -0.8) is a stronger base than LiOH. The other hydroxides, KOH, RbOH, and CsOH, are even stronger bases with pK_b approaching the limiting value of -1.7 for these three hydroxides.

In light of the above, it does not seem reasonable to assign a particular value to the basicity of the Group I metal promoters. Thus, in the following the basicity of the Group I promoters will be compared on a linear scale based on their position in the Periodic Table. When this is done, the catalyst deactivation rate is shown to increase in going down the row position in the Periodic Table (Figure 2). The catalytic activity appears to initially increase in going down the Periodic Table, attain a maximum at K and then decline in going further down the Periodic Table (Figures 11 and 12) at a low space velocity of 10 NL/hr/g-Fe The nearly constant FT rate for all of the promoters is primarily due to the differences in the WGS activity

with Na and K exhibiting a much higher rate that the other promoted catalysts (Figure 13). The selectivity for ethylene, based on ethene and ethane, exhibits the same trend as for CO conversion; thus, the most basic Group I metal oxides exhibit the highest ethylene selectivity (Figure 14). Olefin ratio of C_4 remained stable over different alkali promoted catalyst. Thus, the alkali promoted catalyst that exhibits the highest hydrogenation activity for CO exhibits the lowest hydrogenation activity for ethene. This implies that it is the relative adsorptivity of CO and ethene that determines the hydrogenation activity; based upon this assertion, ethene competes with CO adsorption best with the unpromoted iron catalyst and becomes less competitive as the promoter is located lower in the Periodic Table.

In summary, the relative effectiveness of the Group I alkali metal promoters is not easily defined. In general, potassium promotion provides the superior catalyst from the activity viewpoint for both FTS and WGS reactions. The relative effectiveness of the alkali metal promoters depends upon the level of CO conversion. Furthermore, an iron catalyst that does not contain alkali is more active than catalysts that contain Li, Cs or Rb. Thus, three of the five alkali metals may be viewed, at least at lower levels of CO conversion, as catalyst poisons. Alkali metals show the greatest impact on the selectivity by impacting the fraction of alkene in the C_2 hydrocarbon fraction.

Apart from WGS activity, the basicity of the promoter defines the relative catalytic activity. However, because of the uncertainty of the chemical compound that represents the alkali promoter in the working catalyst and the variety of definitions of basicity, the comparison based on the position in the Periodic Table appears to be as, and perhaps more, reasonable than any of the current basicity scales.

Acknowledgment

This work was supported by U.S. DOE contract number DE-AC22-94PC94055 and the Commonwealth of Kentucky.

REFERENCES

1. H. H. Storch , N. Golumbic and R. B. Anderson, The Fischer-Tropsch and Related Synthesis, John Wiley & Sons, Inc., New York, 1951.
2. G. van der Laan and A. Beenackers, Catal. Rev.-Sci. Eng., 41, 255 (1999).
3. D. Bukur, D. Mukesh and S. Patel, Ind. Eng. Chem. Res., 29 (1990) 194.
4. H. H. Storch, N. Golumbic and R. B. Anderson, "The Fischer-Tropsch and Related Syntheses," John Wiley and Sons, Inc., New York, 1951, p 327.
5. F. Fischer and H. Tropsch, Ges. Abhandl. Kenntis Kohle, 10, 333-501, (1930).
6. M. E. Dry in "Catalysis: Science and Technology," (J. R. Anderson and M. Boudart, Eds.), 1, 155 (1981).
7. M. E. Dry and G. J. Oosthuizen, J. Catal., 11, 18, 1968.
8. M. Röper in "Catalysis in C_1 Chemistry," (W. Keim, Ed.), D. Reidel Pub. Co., Dordrecht, 1983, pp 41-88.
9. B. H. Davis, "Technology Development for Iron and Cobalt Fischer-Tropsch Catalysts," Quarterly Report #1, contract #DE-FC26-98FT40308.
10. A. Raje, R. J. O'Brien, L. Xu and B. H. Davis in Catalyst Deactivation 1997 (C. H. Bartholomew and G. A. Fuentes, eds.), Studies in Surface Science Catalysis, 111, 527 (1997).
11. R. J. O'Brien, L. Xu, R. Spicer and B. H. Davis, Energy & Fuels, 10 (1996) 921.
12. L. Xu, S. Bao, R. J. O'Brien, A. Raje and B. H. Davis, Chemtech., 28 (1998) 47.

13. R. B. Anderson, “The Fischer-Tropsch Synthesis,” Academic Press, New York, 1984.

14. X. Zhan and B. H. Davis, Petrol. Sci. & Tech., 18 (2000) 1037.

15. A. Raje and B. H. Davis, ACS Petrol. Chem. Div. Prepr., 249 (1996).

16. D. W. Smith, J. Chem. Educ., 65, 480-481 (1987).

17. B. Douglas, D. McDaniel and J. Alexander, “Concepts and Models of Inorganic Chemistry,” 3rd Ed., John Wiley & Sons, Inc., New York, 1994.

Table 1

Ranking of Alkali Promoters at Various CO conversion Levels

CO conversion, %	Activity Ranking				
20	Li = K = 1Na = Un*			Rb = Cs = 0.56	
40	K = Na = 1	Un = 0.68	Li = 0.59	Rb = 0.49	Cs = 0.48
60	K = 1	Un = 0.68	Na = 0.64	Rb = 0.34	Cs = Li = 0.28

* = unpromoted catalyst.

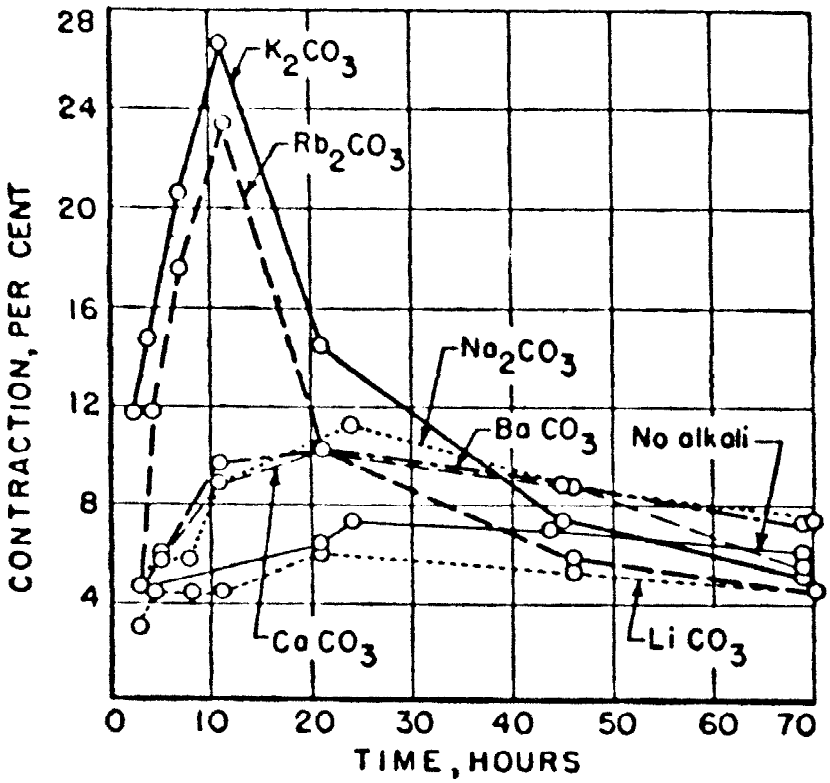

Figure 1. Effect of adding 0.5% alkali on activity of 5 g of Fe-Cu (4:1) catalyst. Reproduced from ref. (5).

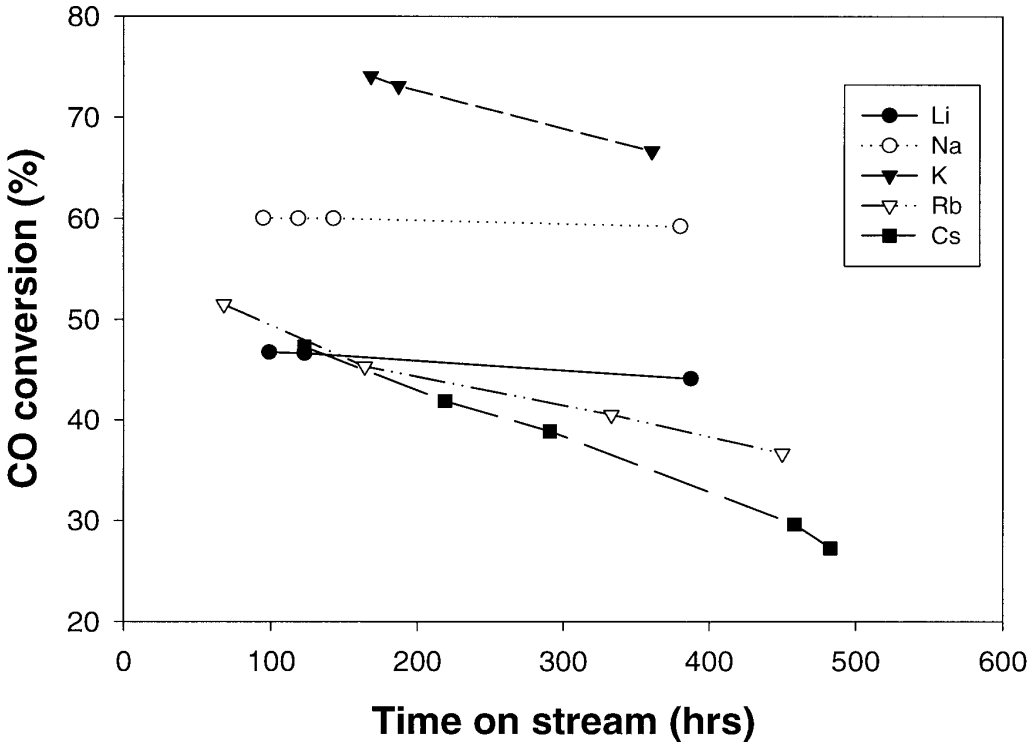

Figure 2. Deactivation curves for Group I alkali metal promoted catalysts established at standard conditions.

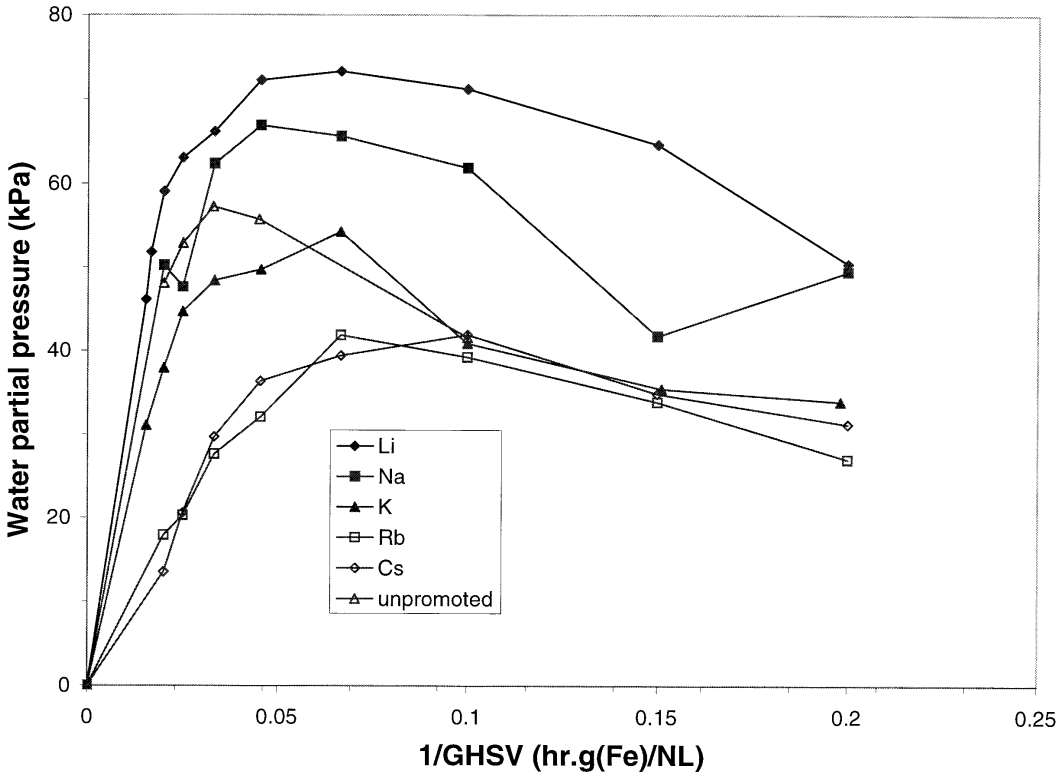

Figure 3. Water partial pressure as a function of space time for iron and promoted iron catalysts.

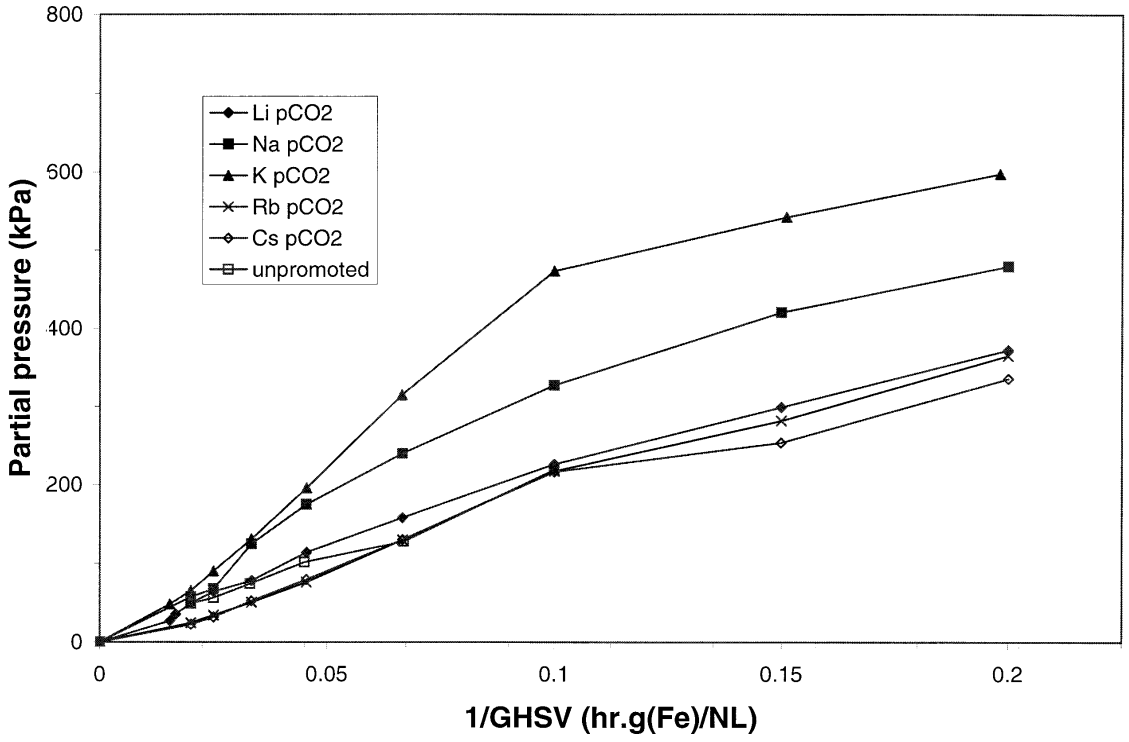

Figure 4. Carbon dioxide partial pressures as a function of space time for iron and promoted iron catalysts.

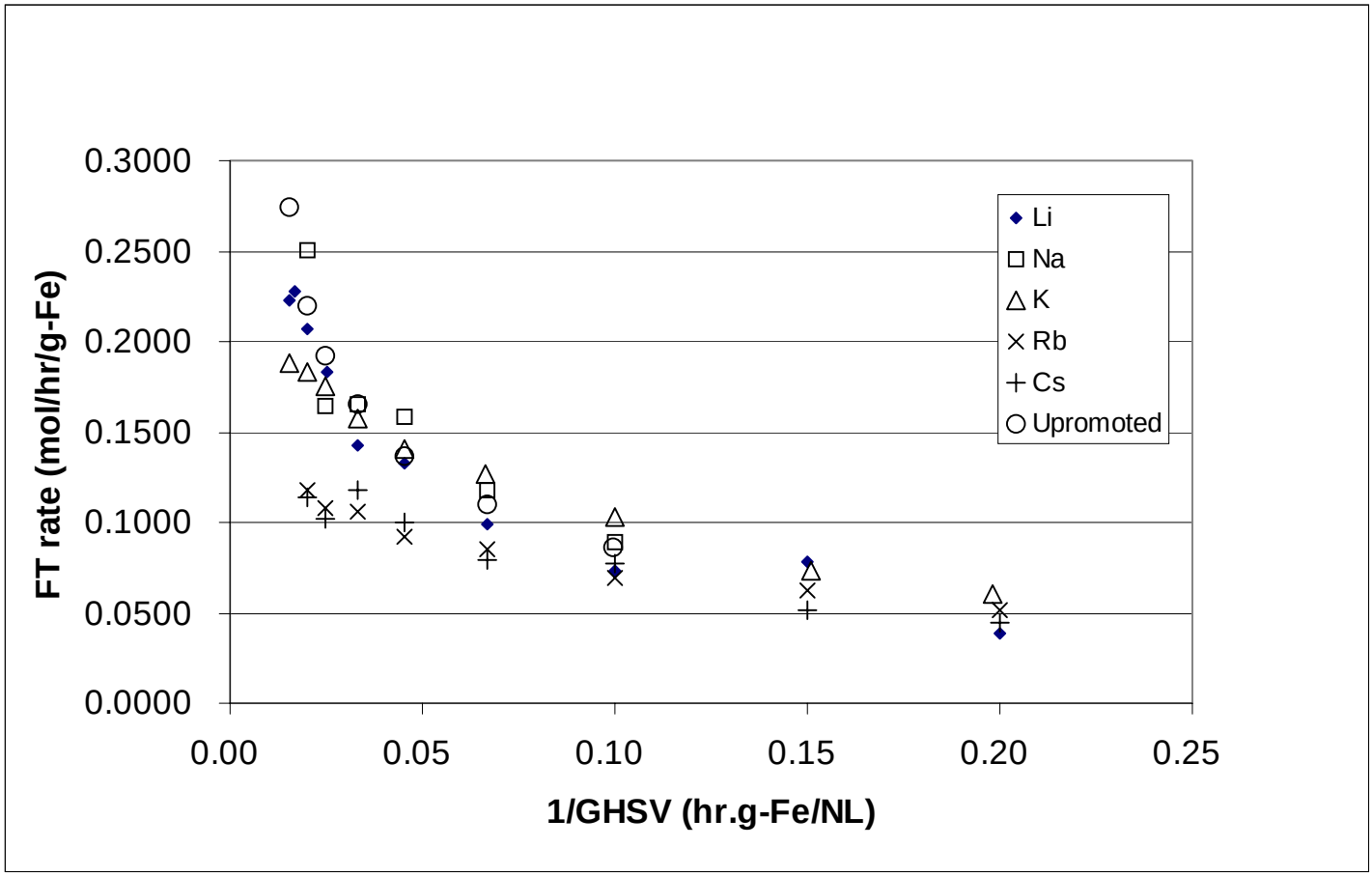

Figure 5. Fischer-Tropsch rate vs. space time.

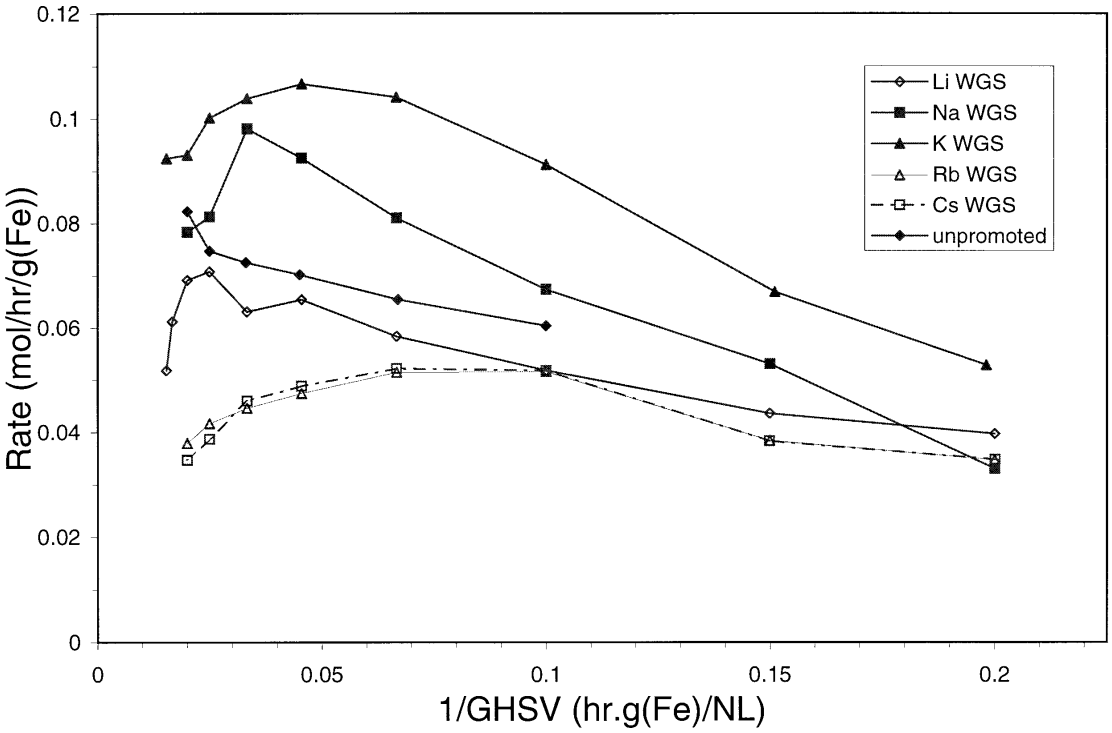

Figure 6. WGS rates as a function of space time for iron and promoted iron catalysts.

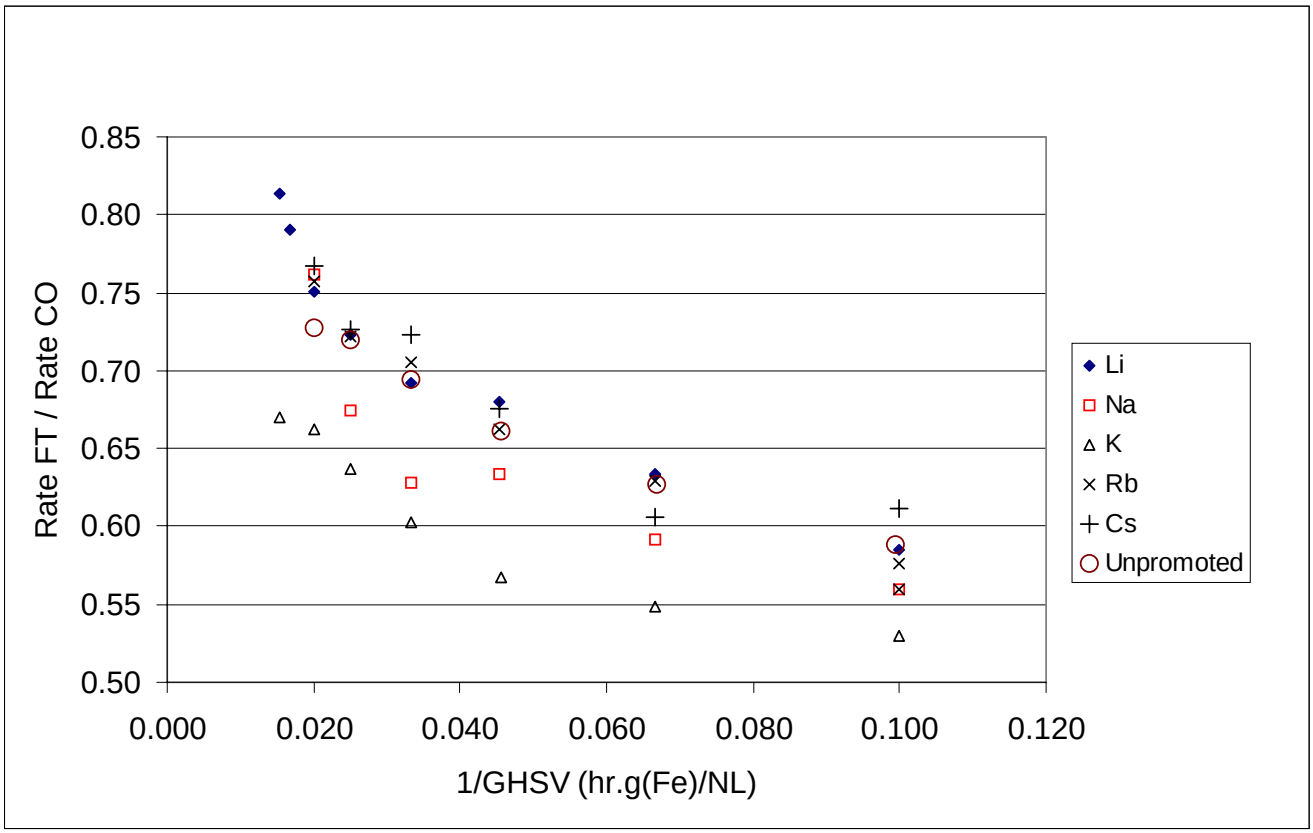

Figure 7. FT to CO rate ratio vs. space time.

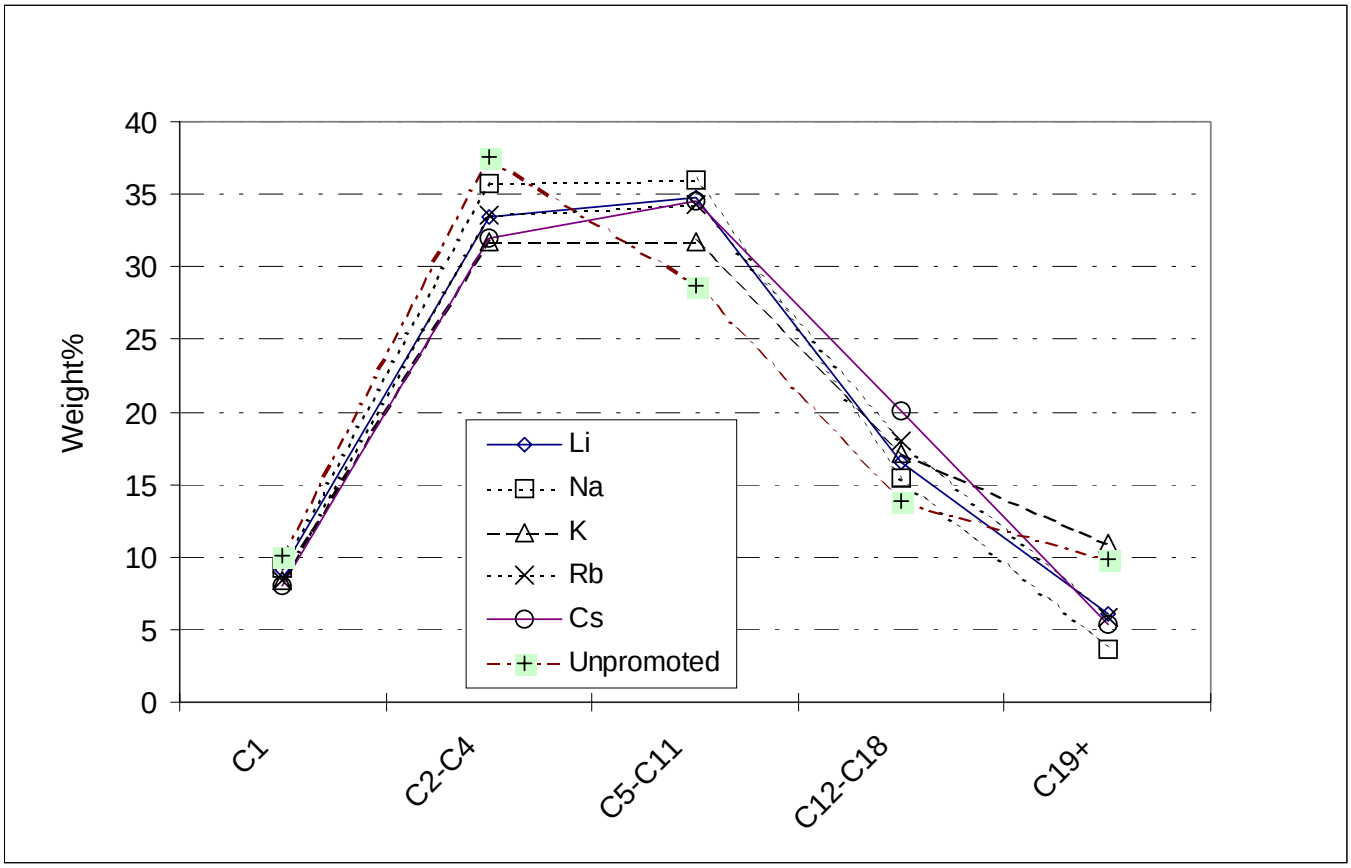

Figure 8. Distributions of hydrocarbon fractions produced using Group I alkali metal promoted catalysts.

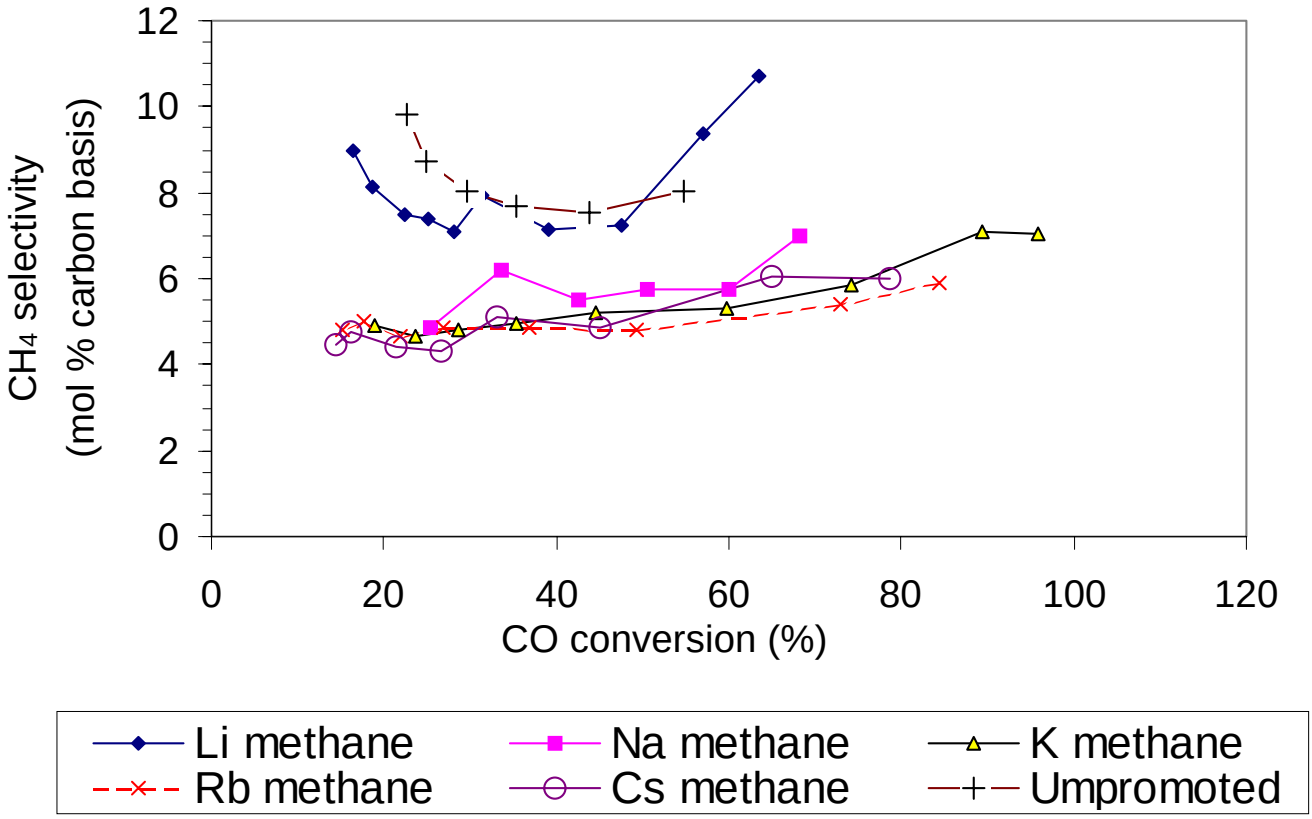

Figure 9. Methane selectivity as a function of carbon monoxide conversion for iron and promoted iron catalysts.

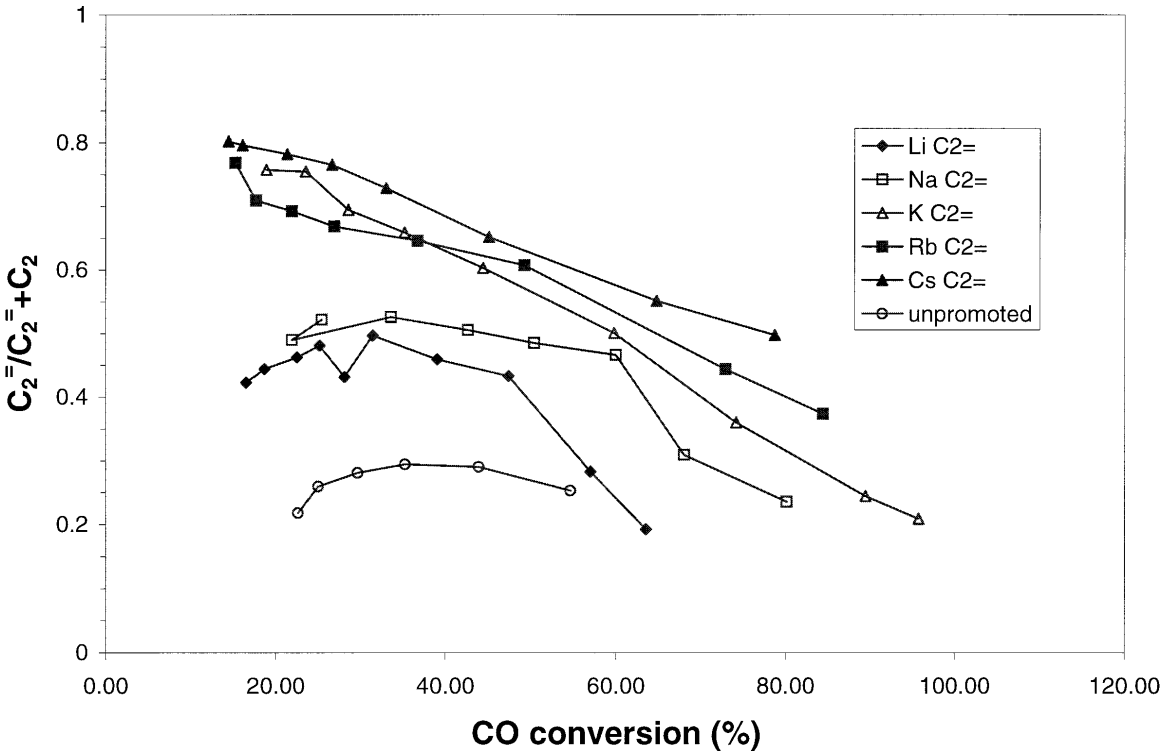

Figure 10. Alkene selectivity of C_2 hydrocarbons as a function of carbon monoxide conversion for iron and promoted iron catalysts.

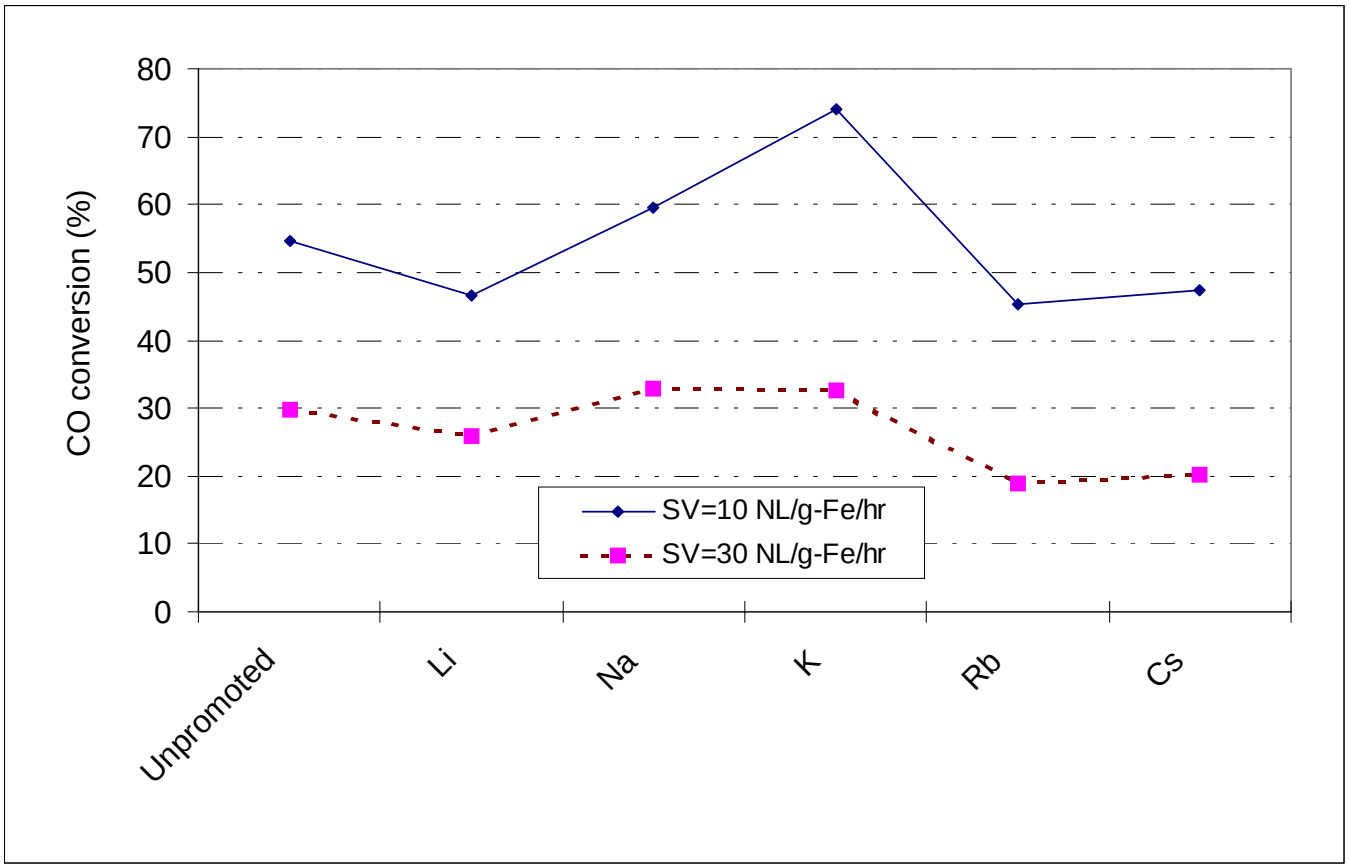

Figure 11. CO conversion vs. alkalinity.

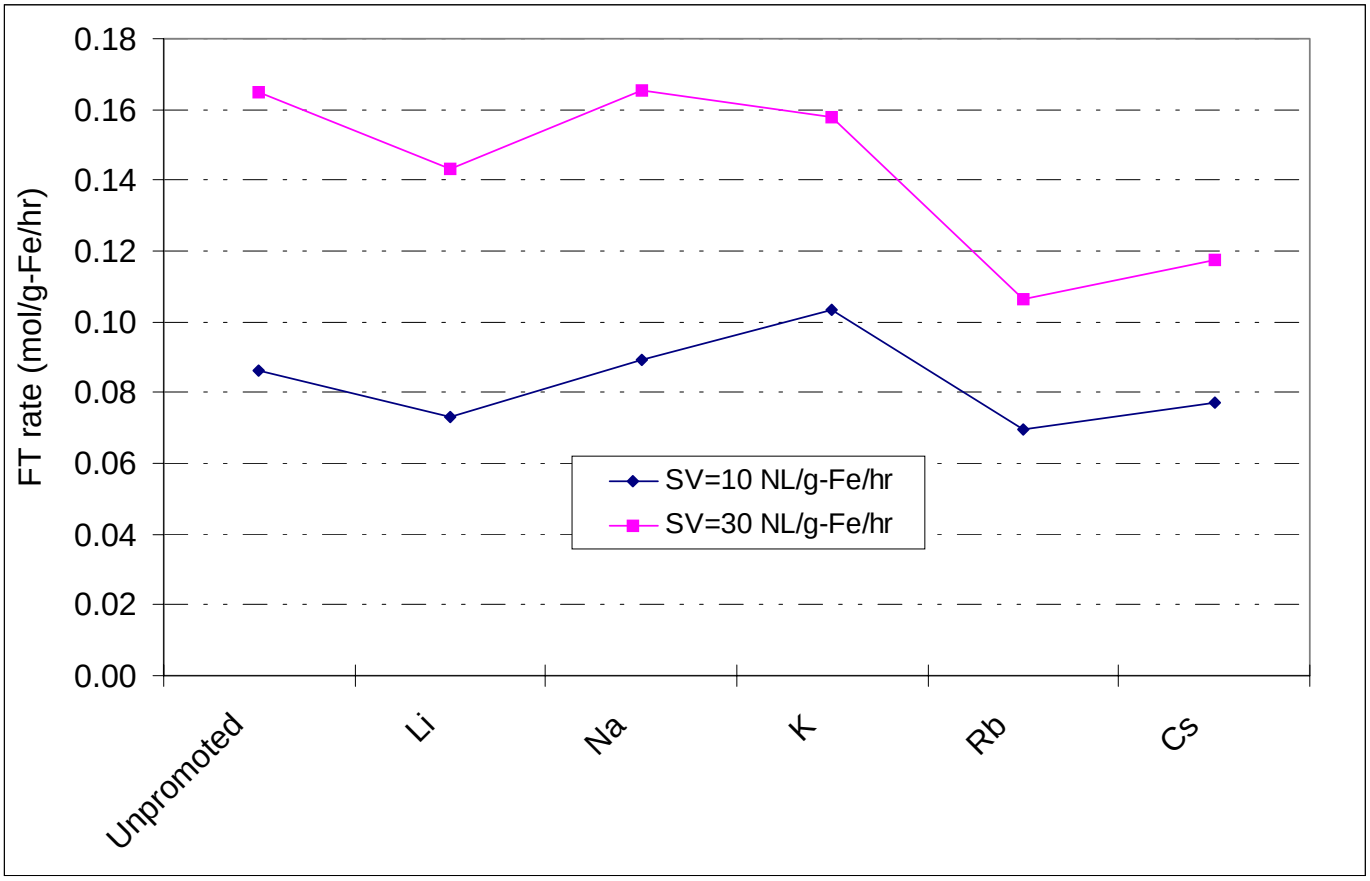

Figure 12. Fischer-Tropsch rate vs. alkalinity.

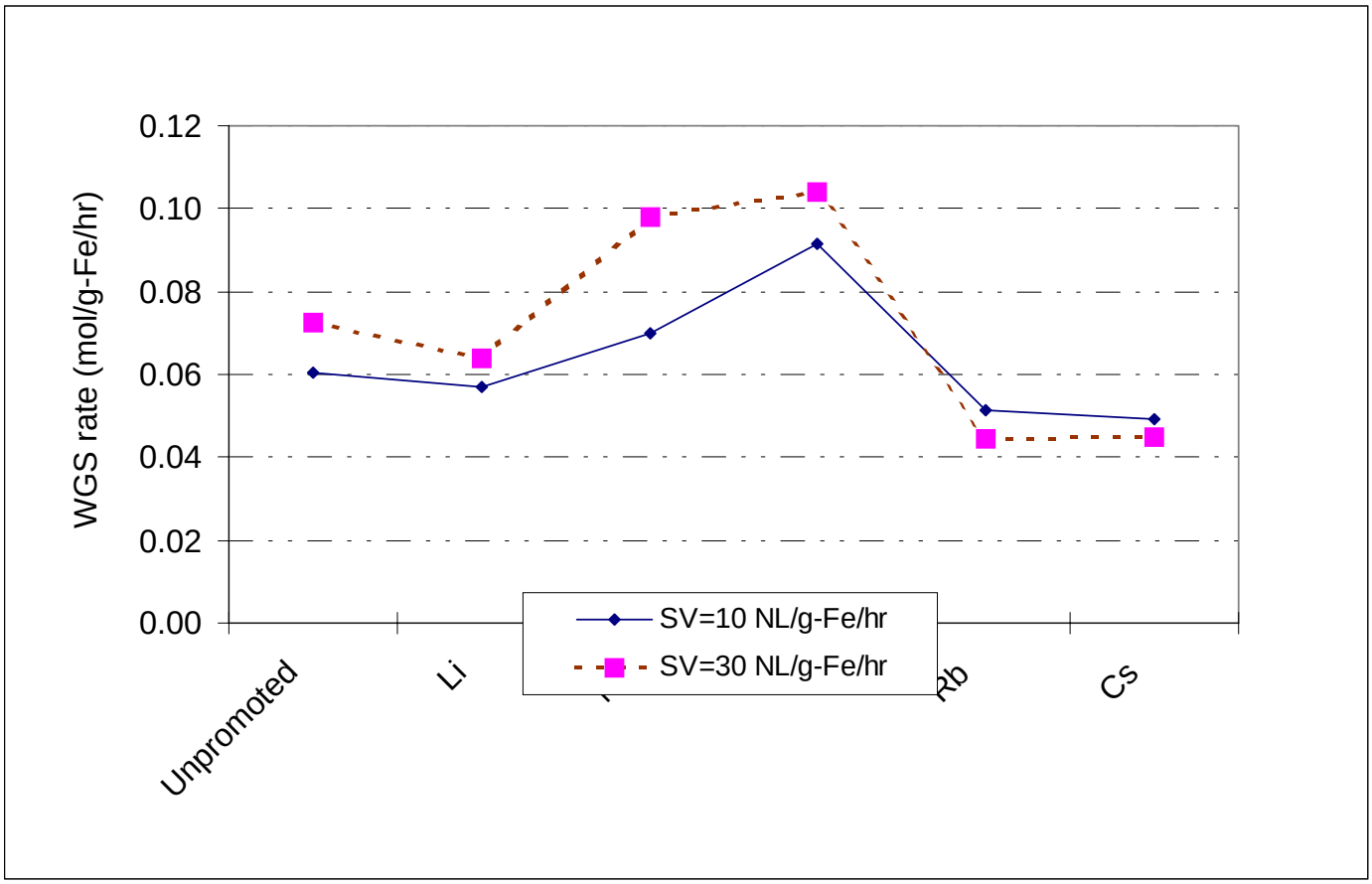

Figure 13. Water-gas shift rate vs. alkalinity.

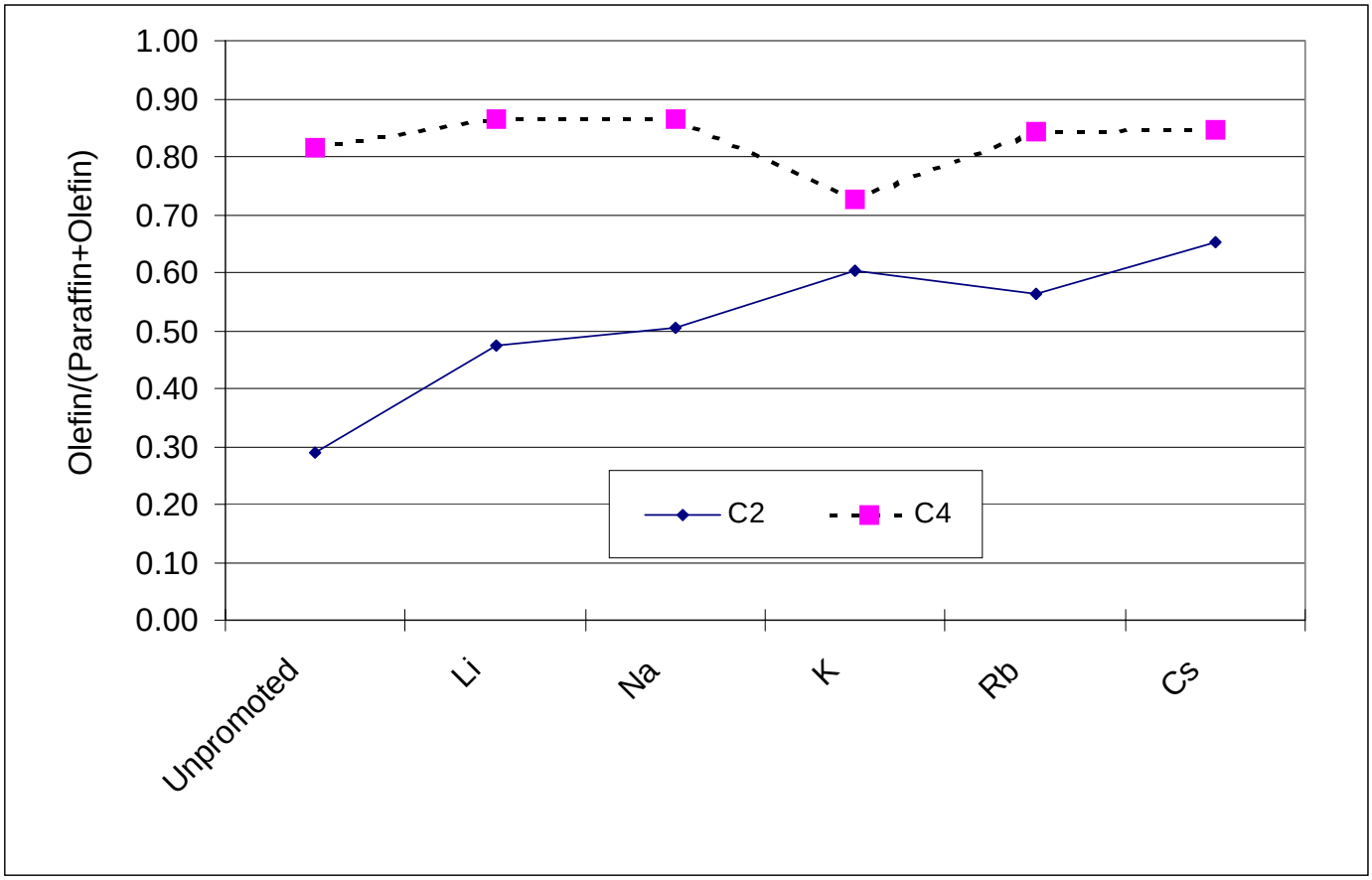

Figure 14. Olefin ratios (C_2 and C_4) vs. alkalinity.

B. Fischer-Tropsch Synthesis: Group II Alkali Metal Promoted Catalysts

Abstract

The effects of four Group II alkali-earth metal (barium, beryllium, calcium and magnesium) and potassium promoters on iron Fischer-Tropsch Synthesis (FTS) catalysts product selectivity, syngas conversion and productivity are compared. Iron FTS catalysts promoted with Group II alkali metals have lower overall FTS activity and lower alpha values than a potassium promoted iron catalyst. All Group II metal promoters yielded higher carbon utilization than a potassium promoted catalyst regardless of the space time. Carbon dioxide selectivity and water-gas shift (WGS) quotient indicate that a potassium promoted iron catalyst possesses better WGS activity than any Group II metal promoted catalyst at high CO conversion. At a low CO conversion, however, K, Ba and Be promoted catalysts produce a similar WGS activity. Among the Group II metals a barium promoted catalyst has the highest WGS activity while a magnesium promoted catalyst showed the lowest WGS activity.

A potassium promoted catalyst generated the highest yield of CO_2 and hydrocarbon but the lowest methane rate. All five catalysts yielded a similar C_3 and C_4 olefin ratio, but a K promoted catalyst produced a notably higher C_2 olefin fraction than Group II metal promoted catalysts. FTS product distributions indicate that a potassium promoted catalyst generated a higher C_{19+} fraction than the other Group II metal promoted catalysts. At a low space time, the potassium promoted catalyst had a lower methane selectivity than Group II metal promoted catalysts but at high space times, all except Ba promoted catalysts had a similar methane selectivity.

Keywords: Fischer-Tropsch synthesis; iron catalyst; promoter, alkali earth metals; barium, potassium, beryllium, magnesium, calcium

Introduction

Fischer-Tropsch synthesis converts a mixture of CO and H_2 that can be produced from coal or natural gas to liquid fuels. One of the advantages of FTS is that the process can be designed to produce gasoline, diesel and/or chemicals. There are two types of operating modes, the low temperature, which is for production of wax, and the high temperature FTS, which is designed for production of gasoline and alkenes.

In FTS process, the hydrocarbon is produced from CO and H_2, which can be expressed as

$$(2n+1)\ H_2 + n\ CO \rightarrow C_nH_{2n+2} + n\ H_2O$$

where n is defined as $n = 1/(1-\alpha)$ or it can be rearranged as $\alpha = 1 - (1/n)$.

When an iron catalyst is used for the FTS reaction, the water gas shift (WGS) reaction can also occur. This side reaction consumes CO and water produced in the FTS process to produce additional hydrogen:

$$H_2O + CO \rightarrow CO_2 + H_2$$

Potassium has long been used as a promoter for iron catalysts to increase the alkene yield and to decrease the CH_4 selectivity [1]. It is also believed that potassium can also increase FTS and water-gas shift catalytic activity [2]. In spite of the widespread use of potassium as a promoter, little work has been reported to allow a direct comparison of promoters at medium or high pressure FTS conditions. We have recently compared potassium to other Group I alkali metal promoters under medium pressure conditions appropriate for slurry reactor operations [3]. The present work extends the work with Group I to include promoters in Group II of the Periodic Table.

Promoted iron FTS catalysts with Fe:alkali-earth metal = 100:1.44 atomic ratio of Group II elements (beryllium, magnesium, calcium and barium) were used in this study. The influence

of alkali-earth on product selectivity, productivity, water gas shift and FTS activity are compared with results obtained from FTS reactions over potassium promoted iron catalyst.

Experimental

Preparation of alkali metal promoted catalysts

Four iron catalysts promoted with Be, Ba, Ca and Mg and one with potassium were prepared and tested in this study. An atomic ratio of 1.44:100 of promoter to iron was used. Precipitated iron catalysts were prepared with tetraethyl orthosilicate, iron nitrate, potassium carbonate and copper nitrate. Ferric nitrate solution was first prepared by dissolving $Fe(NO_3)_3 \cdot 9H_2O$ in distilled and demonize water, and the amount of tetraethyl orthosilicate needed to make Si:Fe of 4.6:100 atomic ratio was added. The mixture was stirred vigorously until the tetraethyl orthosilicate hydrolyzed. The tetraethyl orthosilicate and iron nitrate mixture was then added to a continuous stirred tank reactor (CSTR) precipitation vessel together with a stream of ammonium hydroxide. By maintaining the slurry pH at 9 and an average residence time of 6 minutes, a base catalyst material with an iron to silicon atomic ratio of 100:4.6 was obtained. The slurry was collected using a vacuum drum filter and washed twice with demonize water. The final filter cake was dried in an oven with flowing air at $110^{O}C$ for 24 hours. The catalyst was crushed to approximately 60 μm and calcined for 4 hours in a $350^{O}C$ oven under an air flow.

In this study, the iron catalyst was impregnated with an aqueous nitrate solution of barium, beryllium, calcium or magnesium for alkali-earth metal promoted catalysts, and K_2CO_3 solution for potassium promoted catalyst. Alkali-earth metal or potassium solution was added to obtain a promoter to iron atomic ratio of 1.44:100. Following the impregnation, the catalyst was dried at $110^{O}C$ overnight with good mixing. Thus, catalysts promoted with four Group II alkali-earth metals and one with potassium were prepared for FTS studies.

In-situ catalysts activation

The iron catalyst needs to be activated with either H_2, CO or synthesis gas. Activation procedures can have a significant effect on the selectivity and activity of iron catalyst [4]. It was reported that catalysts activated with CO yielded more long-chain hydrocarbons than syngas and H_2 activated catalysts. In addition, activation conditions may also influence the performance of the iron catalyst. In this study, the potassium promoted iron catalyst was pretreated with CO at 270°C and 1.2 MPa for 24 hours. The reduction of Fe_2O_3 with CO occurs in two steps:

$$3Fe_2O_3 + CO \rightarrow 2Fe_3O_4 + CO_2$$

$$5Fe_3O_4 + 32CO \rightarrow 3Fe_5C_2 + 26CO_2$$

In addition, CO_2 may be formed by the Boudouard reaction:

$$2CO \rightarrow C + CO_2$$

Previous work in our lab showed that, following a 24-hour activation, approximately 50 % to 100% more carbon was present in the catalyst mass than was needed to form Fe_5C_2 [4]. Gradual oxidation of unpromoted Fe_5C_2 to Fe_3O_4 was observed when iron catalyst was used in FTS [4]. The results showed that at the end of the run an unpromoted iron catalysts had been completely oxidized to Fe_3O_4.

Reactor system

A one-liter CSTR was used in this study (Figure 1). A sintered metal filter was installed to remove the wax samples from the catalyst slurry in the reactor. The wax sample was extracted through the internal filter and collected in a hot trap (200°C). The components in the vapor space of the reactor continuously passed to a warm trap (100°C) and cold trap (0°C) that were used to collect samples of oil, light wax and water. Tail gas from the cold trap was analyzed with an HP quick GC.

After the catalyst was activated with CO, syngas was introduced at a rate of 10 NL/hr/gram-catalyst. CO and H_2 were introduced to a gas mixing vessel using mass controllers to provide a simulated synthesis gas. This flow rate was maintained until the activity became constant and was used as the standard reaction condition. Then the gas space velocity was varied in the range of 3 to 60 NL/hr/g-Fe to collect kinetic data. Other reaction conditions were maintained at 270°C, 1.2 MPa and a stirrer speed of 750 rpm.

Product sampling and analysis

Gas, water, oil, light and heavy reactor wax samples were collected daily and analyzed. Table 1 gives the summary of the instruments for gas and liquid product analysis. A heavy wax sample was taken from the 200°C hot trap connected to the filter. Vapor phase above the slurry phase passed to the warm (100°C) and the cold (0°C) traps outside the reactor. The light wax and water mixture was collected from the warm trap and an oil plus water sample from the cold trap. Tail gas from the cold trap was analyzed with an online HP Quad Series Micro GC and molar compositions of C_1-C_7 olefins and paraffins were obtained. Hydrogen and carbon monoxide conversions and CO_2 produced were calculated based on the gas product online GC analysis results and the gas flow measured at the reactor outlet. Hydrogen, carbon monoxide and syngas conversion were obtained using the following formula:

$$\text{Conversion} = \frac{(N_{in} - N_{out})}{N_{in}} \times 100\%$$

The oil and light wax samples were mixed before being analyzed with an HP 5790A GC. The heavy wax was analyzed with an HP5890 Series II Plus GC while the water sample was analyzed with an HP5890 GC.

Results and Discussion

Effect on Fischer-Tropsch synthesis activity

For a synthesis gas of H_2:CO = 0.7:1, Figure 2 shows the results of CO conversion over the catalysts promoted with Group II alkali-earth metals (Ba, Be, Ca and Mg) and potassium. The potassium promoted catalyst yielded the highest overall CO conversion of 70% at the base reaction conditions. The calcium promoted FTS catalyst yielded the lowest initial conversion of 47% while all other Group II alkali-earth metal promoted catalysts produced CO conversions of 50-56% range.

Deactivation rate (%/day) for these five catalysts was obtained from the CO conversion results of over 500 hours of FTS reaction. As described in the experimental section, FTS base reaction conditions were established and then the space velocity was changed from 3 to 50 NL/h/g-iron before the reaction conditions were switched back to the original standard one. Overall deactivation rate was calculated based on the total reaction time; therefore, the overall deactivation rate may be higher than during a run without reaction condition changes. As indicated in Figure 3, beryllium and barium yielded a low deactivation rate of 0.07 and 0.15% per day, respectively, while potassium and calcium were 0.88 and 0.91, respectively. Magnesium promoted catalysts yielded the highest deactivation rate (2.24%/day) among all five catalysts tested. For potassium, this is a faster deactivation rate when the same catalyst is used at one flow rate (3.1 NL/hr gcat) and a high (90%) initial CO conversion. Presumably altering the reaction conditions causes a higher deactivation rate.

Figure 4 shows the results of CO conversions at various space velocities (NL/g-Fe/h) (space time = h•g-Fe/NL) following establishment of stable activity at the base condition. At low space time, all Group II alkali-earth metal promoted catalysts produced a CO conversion similar to the potassium promoted catalyst. At an intermediate range of space time, however, the

catalysts showed different CO conversions. Potassium yielded the highest overall CO conversion at both a high and a medium space time. At a high space time, magnesium yielded a similar conversion to potassium. Both beryllium and barium showed nearly the same CO conversion in the full range of the space time of 3 to 50 h•g-Fe/NL. Calcium produced the lowest CO conversion at a space time above 0.1 h•g-Fe/NL, and showed the lowest activity at a high space time.

Effect on Fischer-Tropsch synthesis selectivity

Figures 5 and 6 show the rates of hydrocarbon, methane, CO_2 and water formation for FTS reactions catalyzed with Group II alkali-earth metal and potassium promoted catalysts under the reaction conditions (270˚C, 175sig and H_2:CO of 0.67:1) at the same low CO conversion (20%). All Group II alkali-earth metal promoted catalysts produced a higher hydrocarbon rate than the potassium promoted catalyst at this CO conversion. A 3.2 to 3.7 g/h/g-iron hydrocarbon rate was obtained for Group II alkali-earth metal promoted catalysts while the potassium promoted catalyst generated a lower hydrocarbon rate of 2.75 g/h/g-iron. Figure 6 shows that the rate for methane production for the potassium promoted catalyst was lower than all Group II alkali-earth metal promoted catalysts. While the potassium promoted catalyst produced a similar CO_2 rate to that of Be and Ba, it yielded a lower water production rate than other Group II alkali-earth metal promoted catalysts. This result shows that the potassium promoted catalyst generated a higher WGS activity than Group II alkali-earth metal promoted catalysts. The data in Figure 6 also show that calcium and magnesium promoted catalysts produced lower CO_2 rates than other alkali-earth metal promoted catalysts.

Olefin ratio was calculated from the following equation:

$$\text{Olefin ratio} = \frac{Olefin}{(Olefin + Paraffin)}$$

Figure 7 shows the olefin ratio from FTS over potassium and Group II alkali-earth metal promoted iron catalysts compared at the same 20% CO conversion. The data show that all Group II alkali-earth metal and potassium promoted catalysts yielded similar C_3 and C_4 olefin ratios that fall in the 0.85-0.90 range. Ethene fraction, however, shows a significant difference between potassium and Group II alkali-earth metal promoted catalysts. An ethene fraction of 0.76 was obtained for the C_2 fraction for the potassium promoted catalyst while an ethene fraction of 0.30-0.35 was obtained for the Group II alkali-earth metal promoted catalysts.

The distribution of hydrocarbon fractions (Figure 8) show that potassium produced more C_{19+} than the Group II alkali-earth metal promoted catalysts. The potassium promoted catalyst produced a similar amount of C_{12}-C_{18} fraction as the Be and Ca promoted catalysts but a smaller gasoline fraction (C_5-C_{11}) than the Group II alkali-earth metal promoted catalysts. Among the Group II alkali-earth metal promoters, Ca produced the largest gasoline fraction (44.9%) and the smallest gas (C_1-C_4) and C_{19+} fraction while the Ba promoted catalyst generated the highest C_{19+} and C_1-C_4 fractions.

Figure 9 shows the CO_2 selectivity obtained from FTS reactions catalyzed by Group II alkali-earth metal promoted catalysts. In this study, space time varied in the range of 0.02 to 0.33 hr-g(Fe)/l, i.e., space velocities in the range of 3 to 50 NL/h/g(Fe). The potassium promoted catalyst produced more CO_2 than any alkali-earth metal promoted catalyst in the whole range of space time although the CO_2 selectivity trends converge at a space time of about 0.1. Magnesium and calcium promoted catalysts produced a lower CO_2 yield than beryllium and barium promoted catalysts. At a low space velocity, the barium promoted catalyst generated the most CO_2 while all the other Group II alkali-earth metal promoted catalysts produced a similar CO_2 selectivity (40-42%). Therefore, calcium and magnesium promoted catalysts gave better carbon utilization than beryllium and barium promoted catalysts. The potassium promoted

catalysts produced a lower carbon utilization than any of the Group II alkali-earth metal promoted catalysts. Higher CO_2 production from the potassium promoted catalyst suggests that it had a better WGS activity.

As another measure of carbon utilization, methane selectivity is shown in Figure 10. Although the potassium promoted catalyst produced the most CO_2, it generated the least methane at high space velocity among the five catalysts tested in this study. Except at a low space velocity, all Group II alkali-earth metal promoted catalysts generated similar amounts of methane.

Over the range of CO conversion (space time range), the potassium promoted catalyst provided a lower water partial pressure than the other promoted catalysts (Figure 11). Even so, all of the promoted catalyst produced the maximum water partial pressure at about the same space time (0.05; 40-50% CO conversion).

The carbon usage ratio (fraction of CO converted to hydrocarbons) was lower for the potassium promoted catalyst than for the Group II alkali-earth promoted catalysts. The utilization ratio for the four alkali-earth promoted catalysts are similar (Figure 12).

The alpha values obtained for the promoted catalyst are summarized in Figure 13. The potassium promoted catalyst had the largest alpha value, 0.80. There was a gradual decline in alpha for the alkali-earth promoted catalysts as the promoter was located lower in the Periodic Table, attaining 0.75 as the lowest value.

Conclusion

Iron FTS catalysts promoted with Group II alkali-earth metals produced lower overall FTS activity and lower alpha values than a potassium promoted iron catalyst. The lowest alpha values were obtained from Ba and Ca promoted catalysts. Among the Group II alkali-earth metals, Mg and Ba promoters caused slightly higher FTS activity than Be and Ca promoted

catalysts. The catalytic activity of the potassium promoted catalyst declined more rapidly when the conditions were changed than when operating at the same temperature, pressure and 3.1 NL/hr gFe (90% CO conversion initially). Ba and Be promoted catalysts showed better stability than the potassium and calcium promoted catalysts which were more stable than the magnesium promoted catalyst. All Group II alkali-earth metal promoted catalysts yielded a higher carbon utilization than the potassium promoted catalyst regardless of the space time.

Carbon dioxide production shows that the potassium promoted catalyst possesses better WGS activity than any Group II alkali-earth promoted catalyst, even at a high CO conversion. At a low CO conversion, however, K, Ba and Be promoted catalysts had similar WGS activity. Barium promotion generated the highest WGS activity while magnesium promotion showed the lowest WGS activity among the Group II alkali-earth metals. The higher WGS activity for the potassium promoted catalyst led to a lower carbon utilization rate than for the Group II alkali-earth promoted catalysts.

Although the C_3 and C_4 olefin/paraffin ratio did not vary with promoter, a notably higher C_2 olefin/paraffin ratio was obtained for the potassium promoted catalyst than for the Group II alkali-earth promoted catalysts. The yield of various hydrocarbon product fractions varied only slightly among the promoted iron catalysts.

Acknowledgment

This work was supported by U.S. DOE contract number DE-FC26-98FT40308 and the Commonwealth of Kentucky.

References

1. M. E. Dry, in Catalysis Science and Technology (J. Anderson and M. Boudart, eds.), Vol. 1 (1981) 159-255.
2. D. B. Bukur, D. Mukesh, and S. A. Patel, Ind. Eng. Chem. Res., 29 (1990) 194.
3. N. H. Wilfried, Y. Zhang, R. J. O'Brien and B. H. Davis, "Fischer-Tropsch Synthesis: Activity and Selectivity for Group I Alkali Promoted Iron-Based Catalysts," Appl. Catal. A: Gen., in press.
4. R. J. O'Brien, Y. Zhang, H. H. Hamdeh, B. H. Davis, Preprints, ACS Div. of Pet. Chem., 44, 100-102 (1999) March 21-25, Anaheim, CA.
5. R. J. O'Brien, L. Xu, R. L. Spicer and B. H. Davis, Energy and Fuels, 10 (1996) 921.

Table 1 Analyzers for FTS Products		
Analyzer	Sample	GC Detector
HP Quad Series Micro GC	Gas	TCD
HP 5890A Series II	Water	TCD
Agilent 6890	Oil + Light Wax	FID
HP 5890 Series II Plus	Heavy Wax	FID

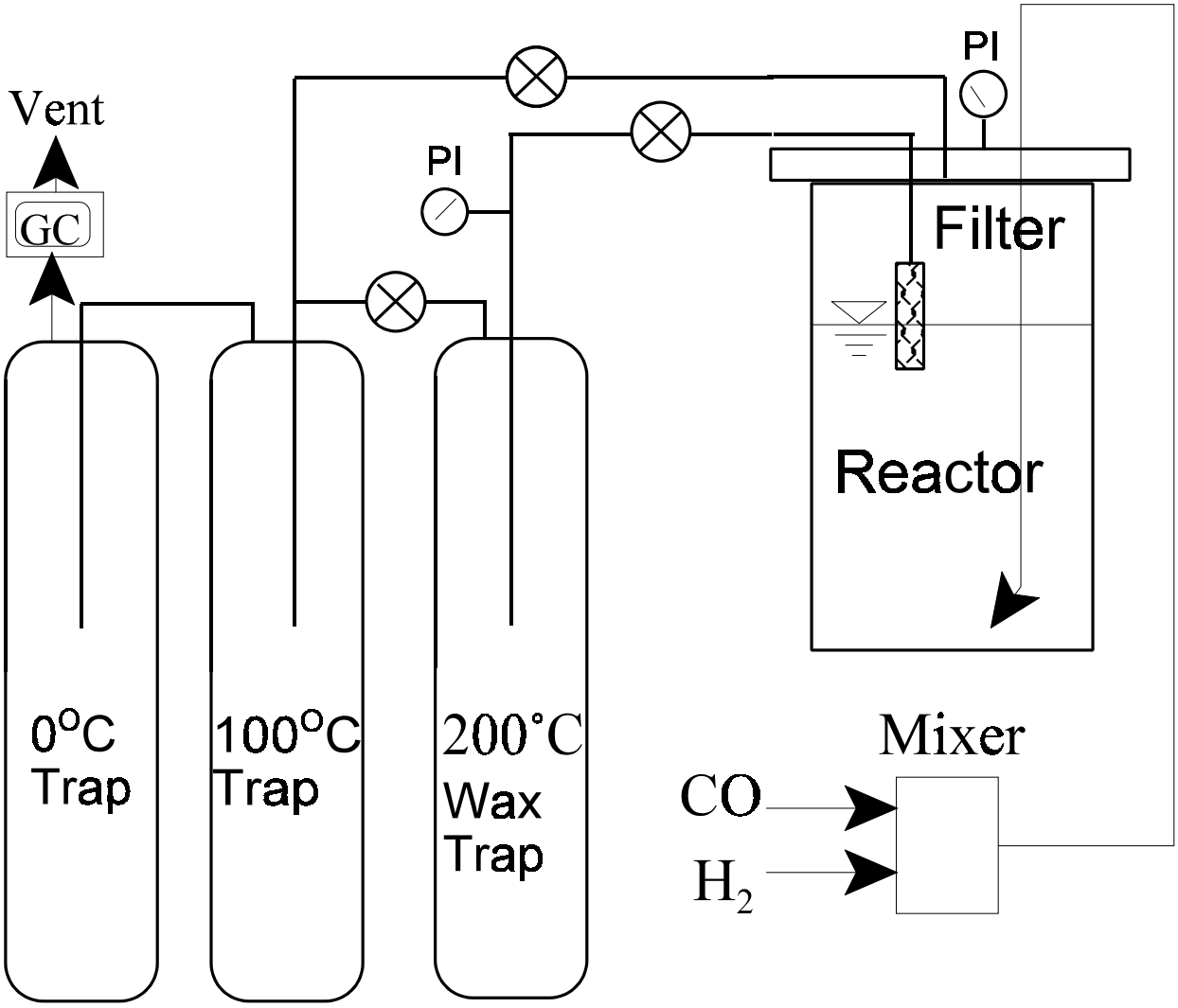

Figure 1. CSTR Fischer-Tropsch system reactor system.

Figure 2. Effect of promoter on iron FTS catalyst activity (270°C, 1.2 Mpa and 10 sl/h/g-iron)

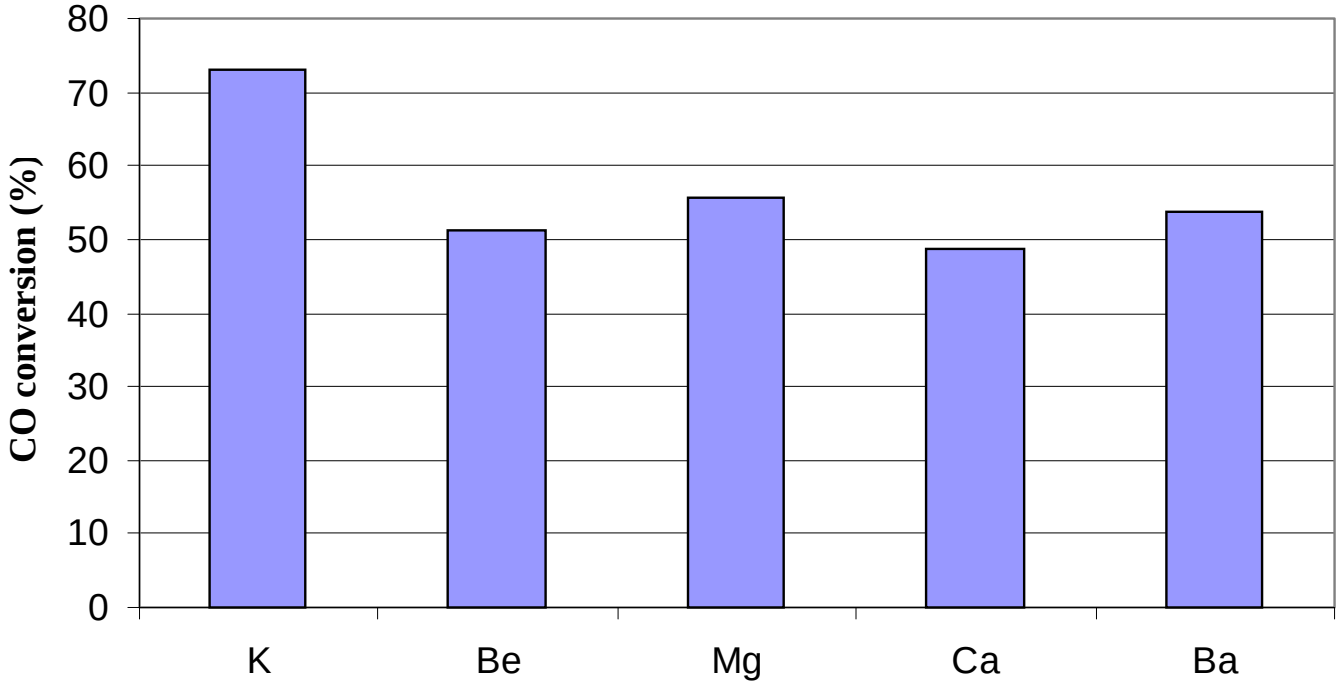

Figure 3. Deactivation Rate of potassium and alkali earth promoted catalysts (270°C, 1.3MPa, 10NL/h/g-iron)

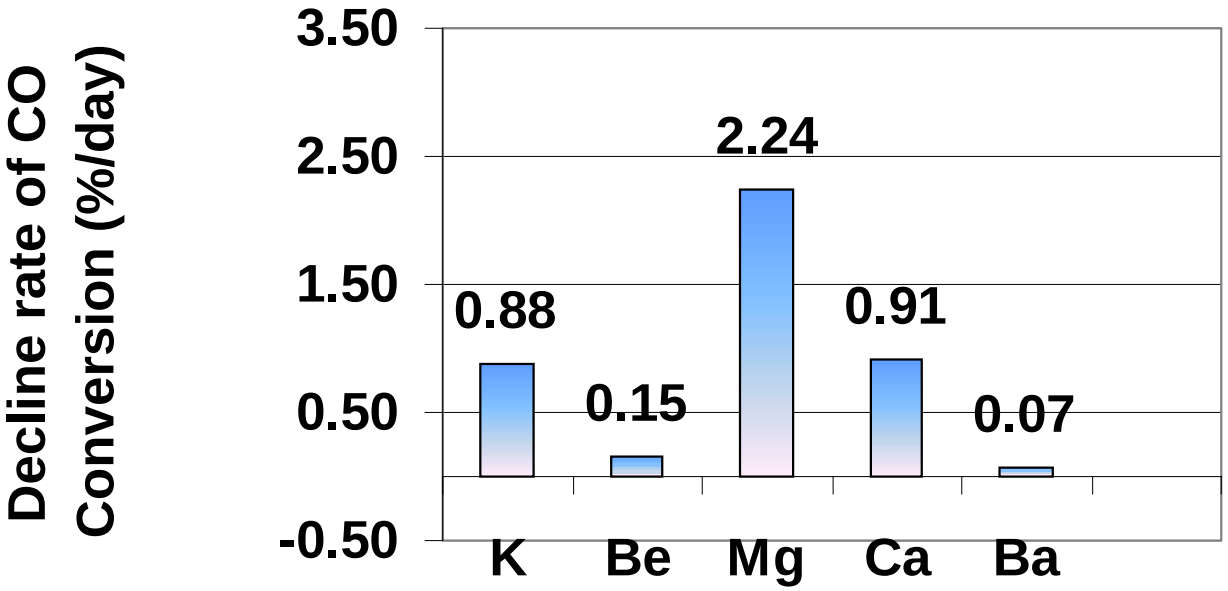

Figure 4. Effect of alkali promoter on CO conversion
(270°C, 1.2 MPa)

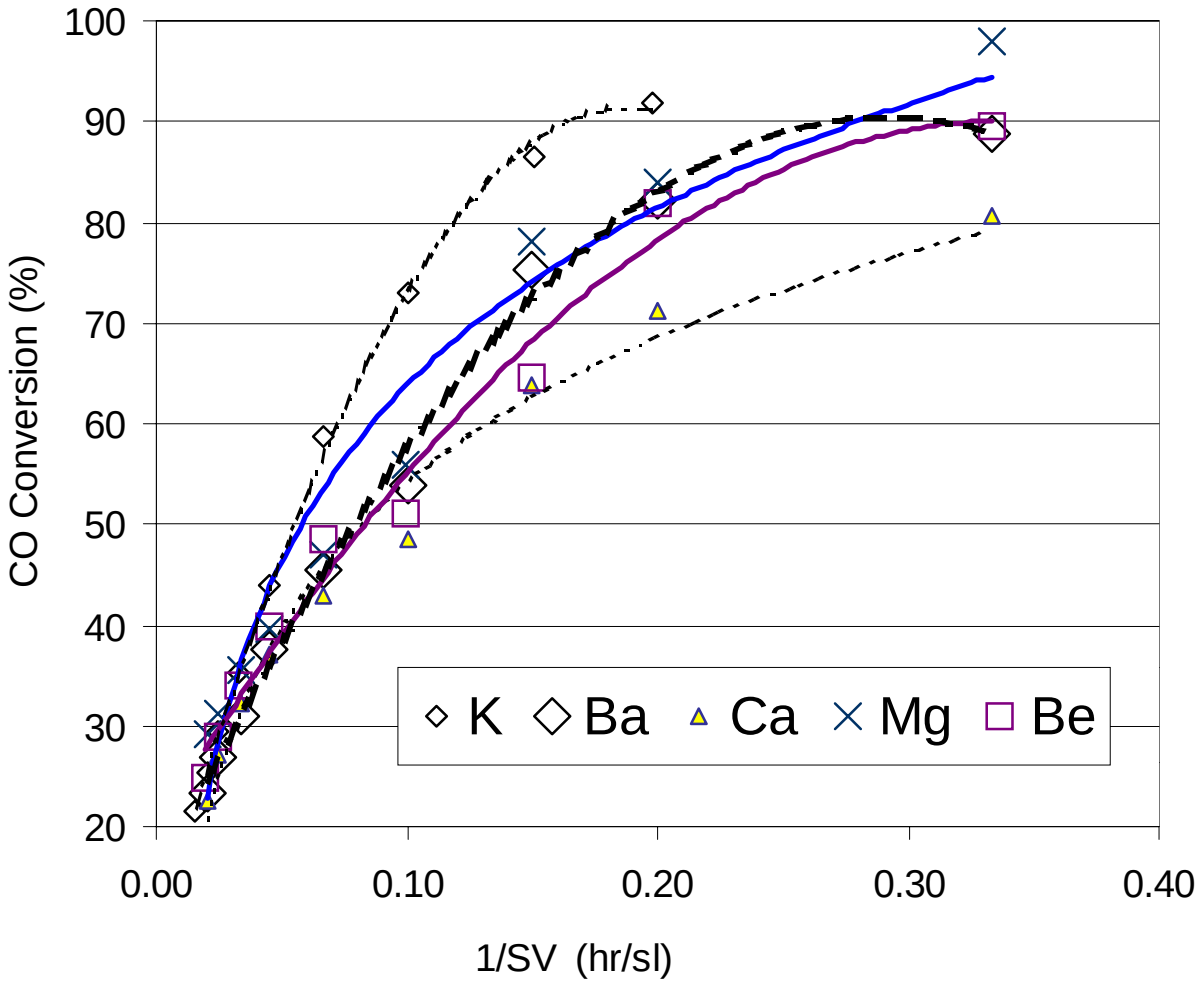

Figure 5. Hydrocarbon rate at 20% CO conversion

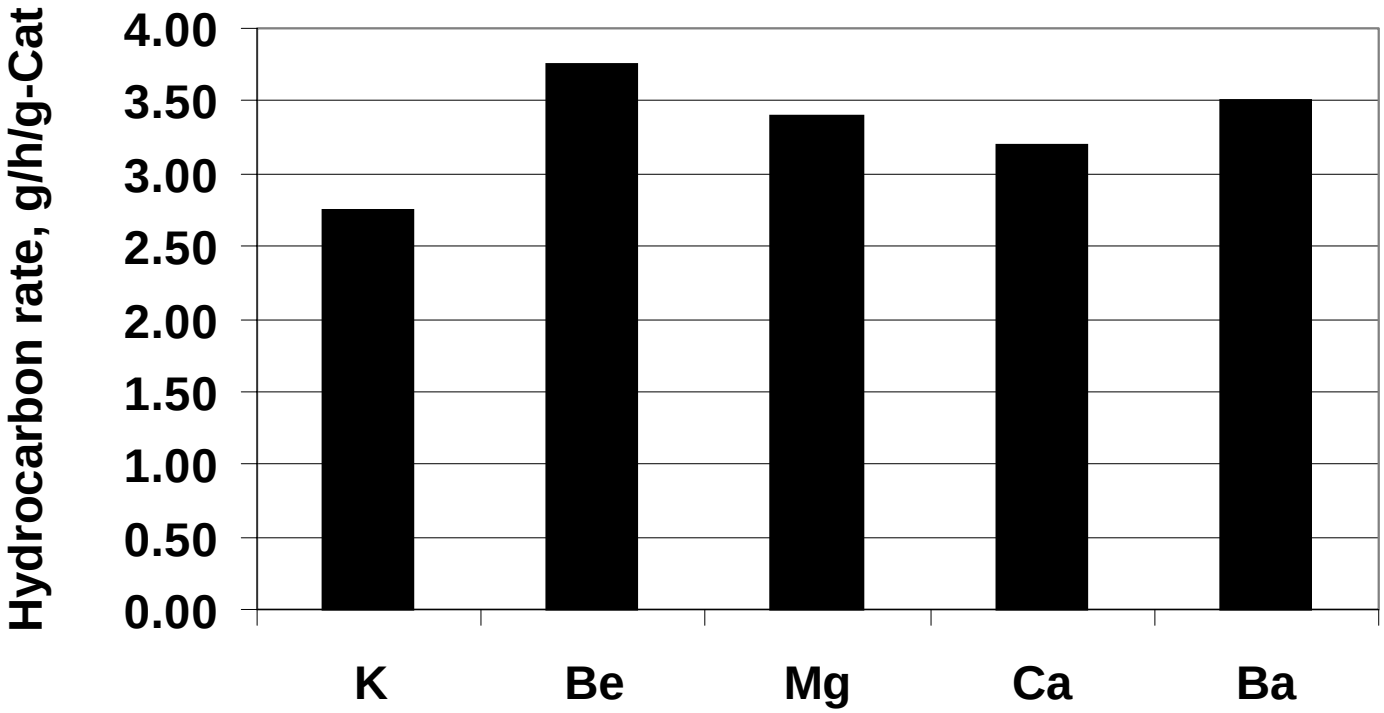

Figure 6. Production of CO_2 H_2O and CH_4 at 20% CO conversion

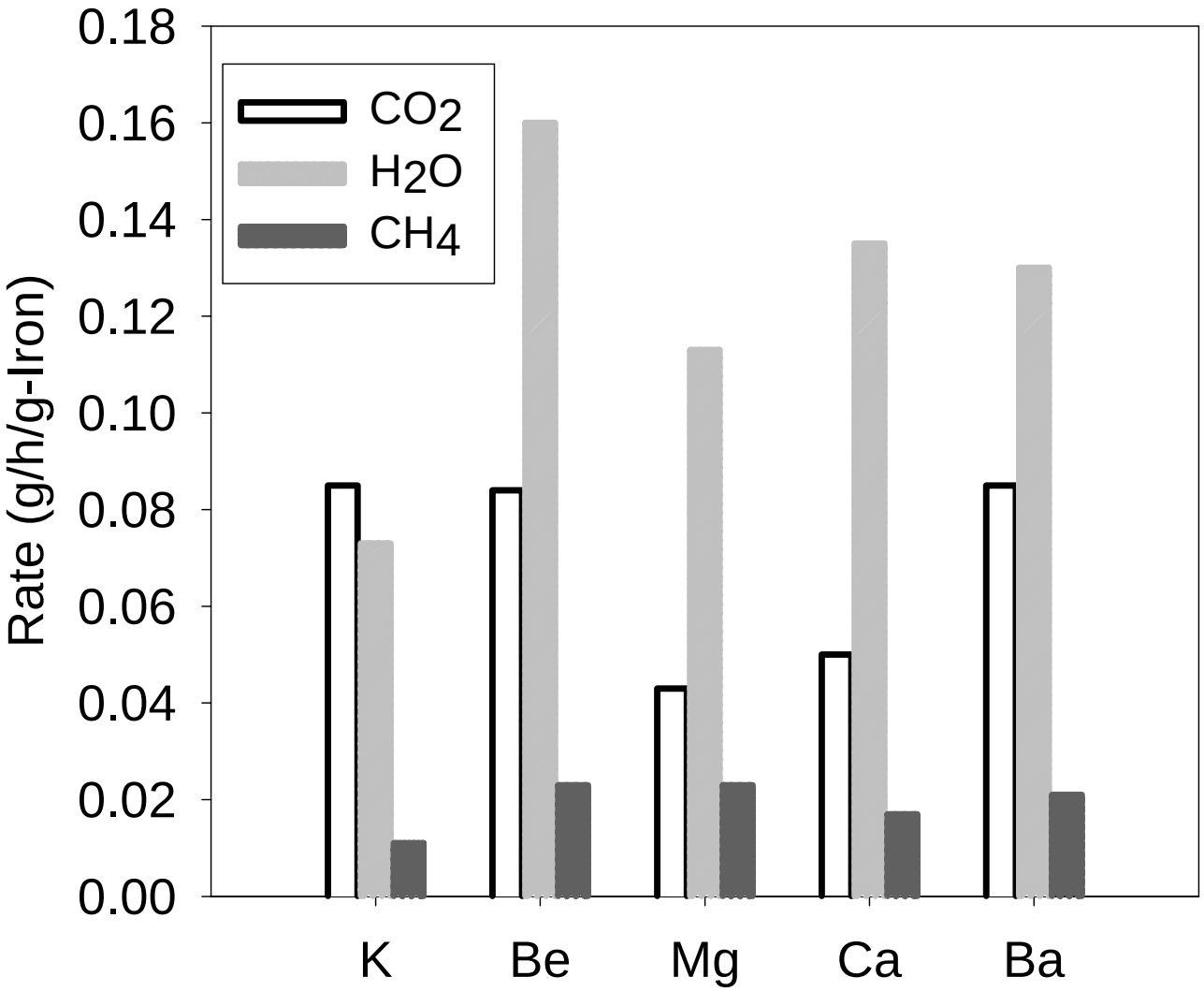

Figure 7. Effect of alkali promoters on olefin ratios at 20% CO conversion

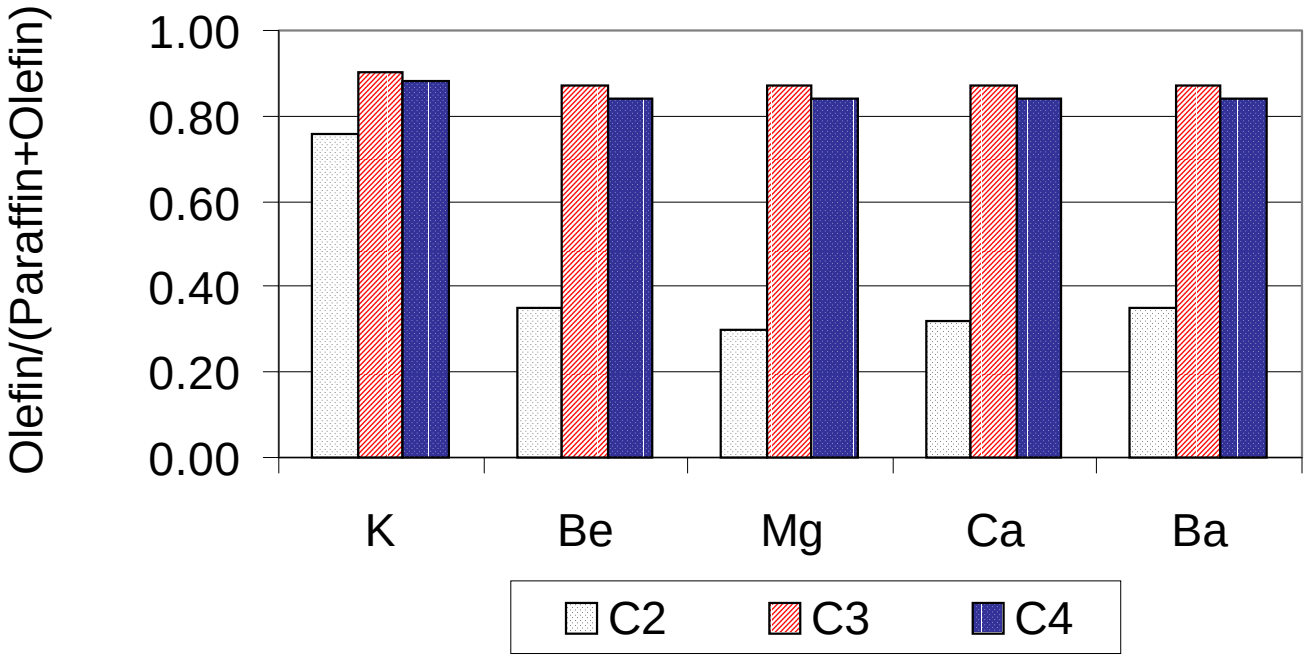

Figure 8. Effect of promoters on hydrocarbon distribution at 20% CO conversion

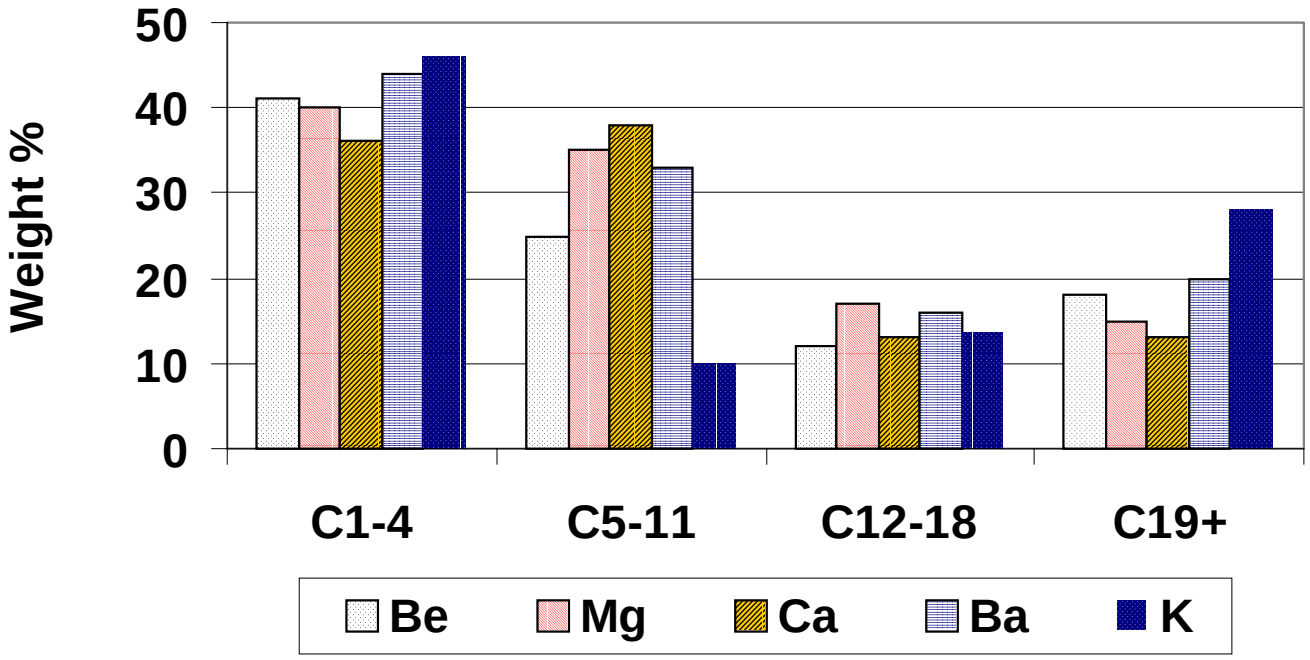

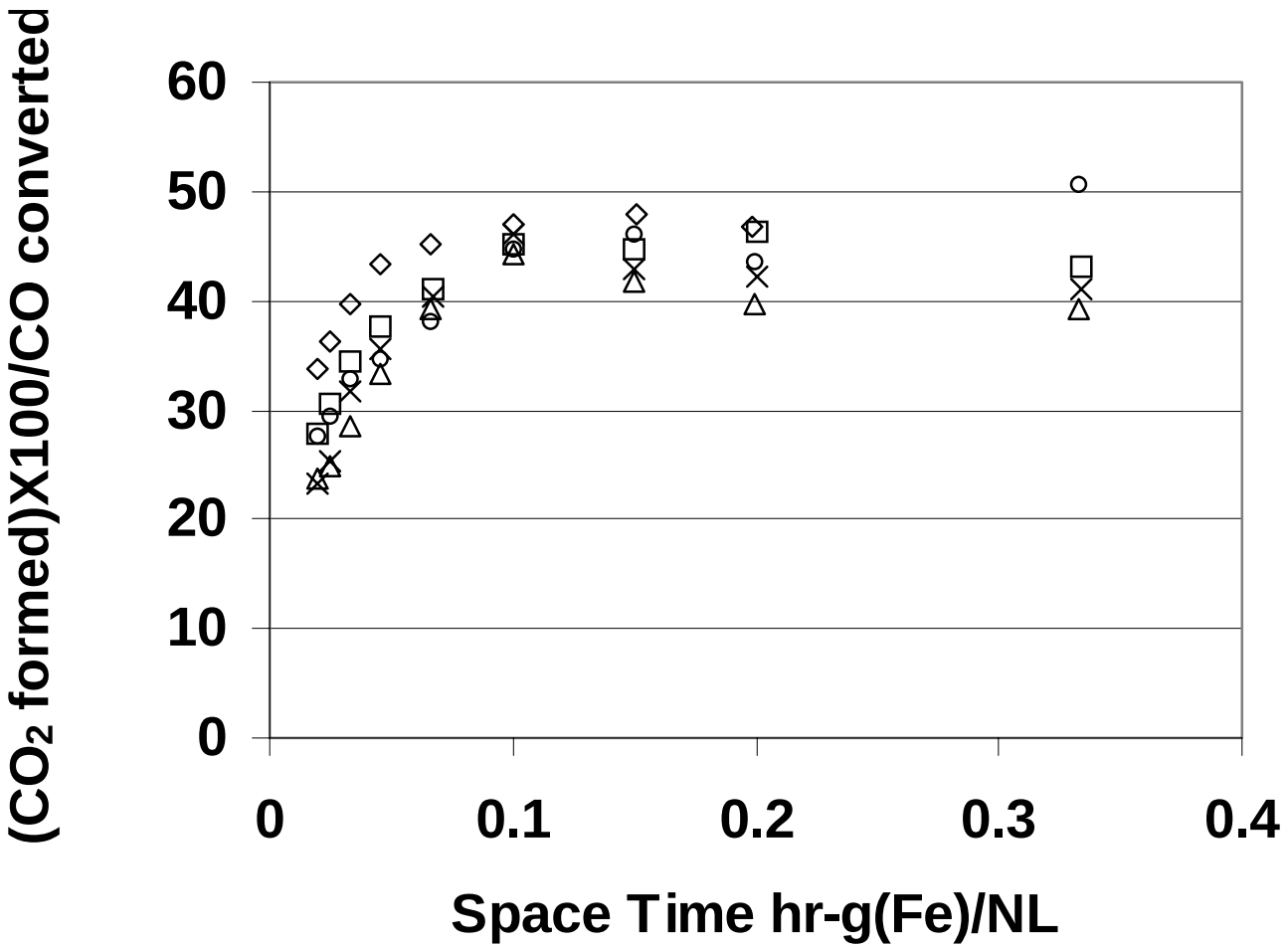

Figure 9. Influence of alkali nature on CO_2 selectivity (♢, K; □, Be; Δ, Mg; x, Ca; ", Ba).

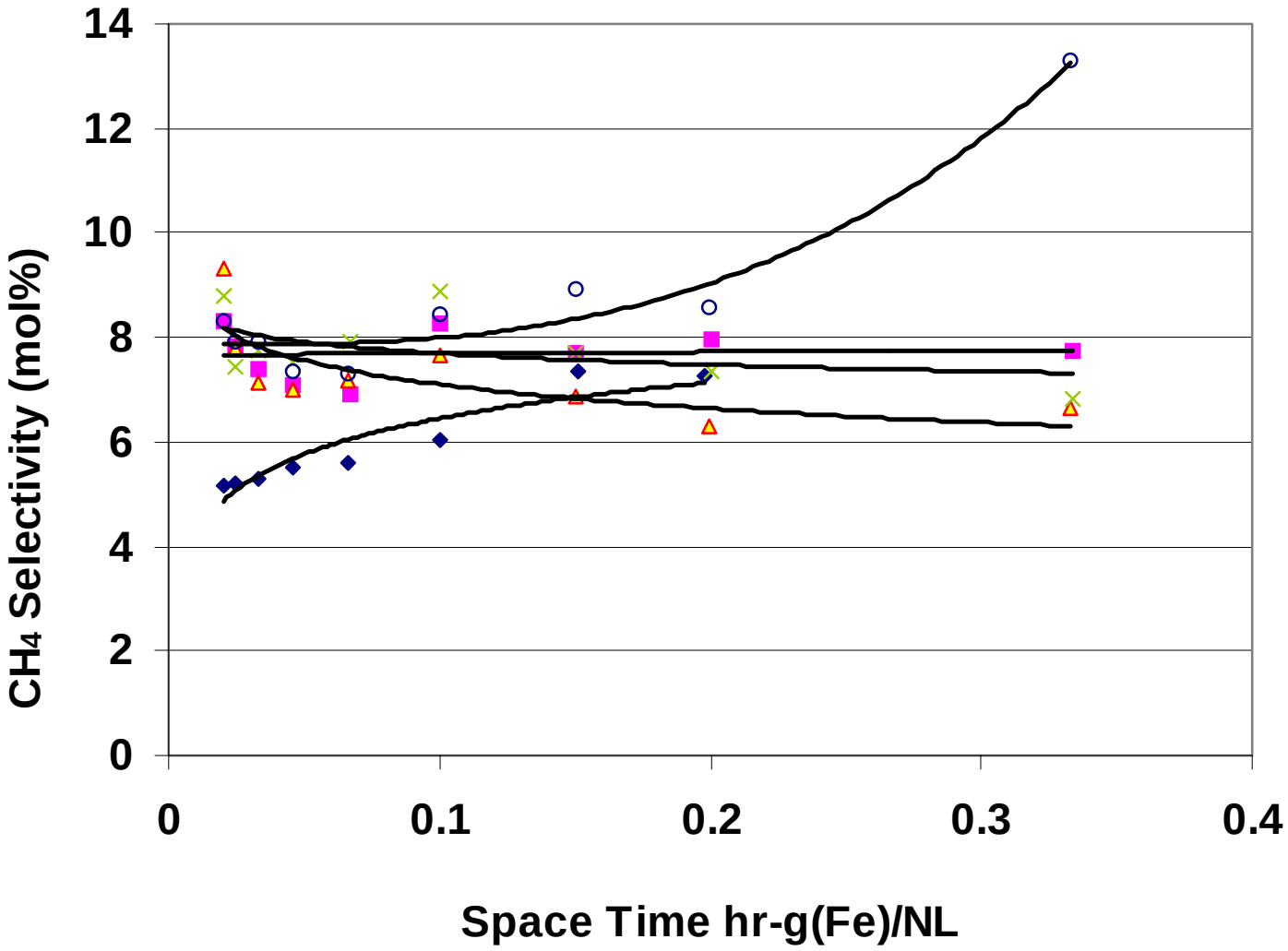

Figure 10. Alkali nature on methane selectivity (◆, K; ■, Be; ▲, Mg; x, Ca; ", Ba).

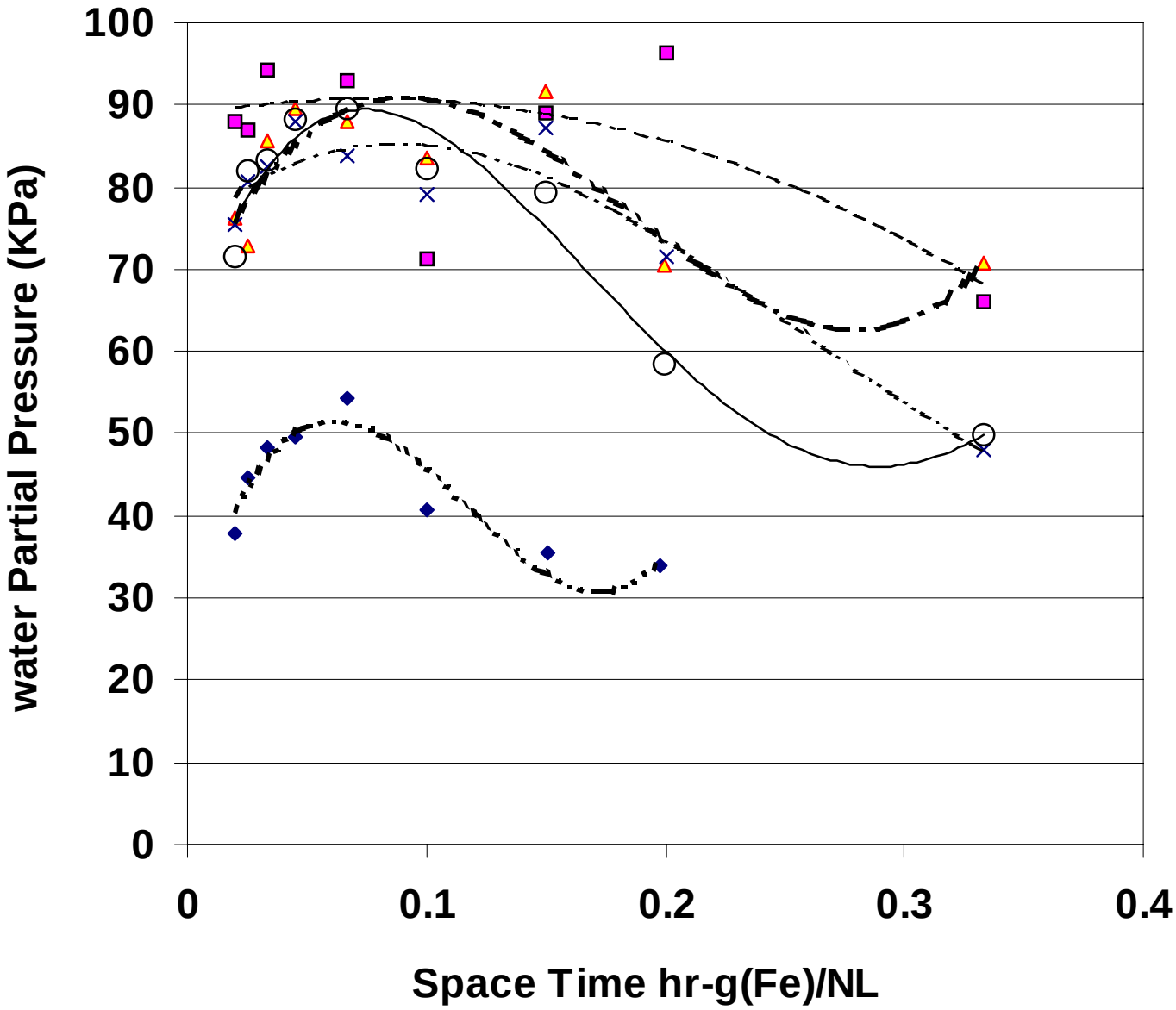

Figure 11. Effect of the promoter on the water partial pressure (◆, K; ■, Be; ▲, Mg; x, Ca; " , Ba).

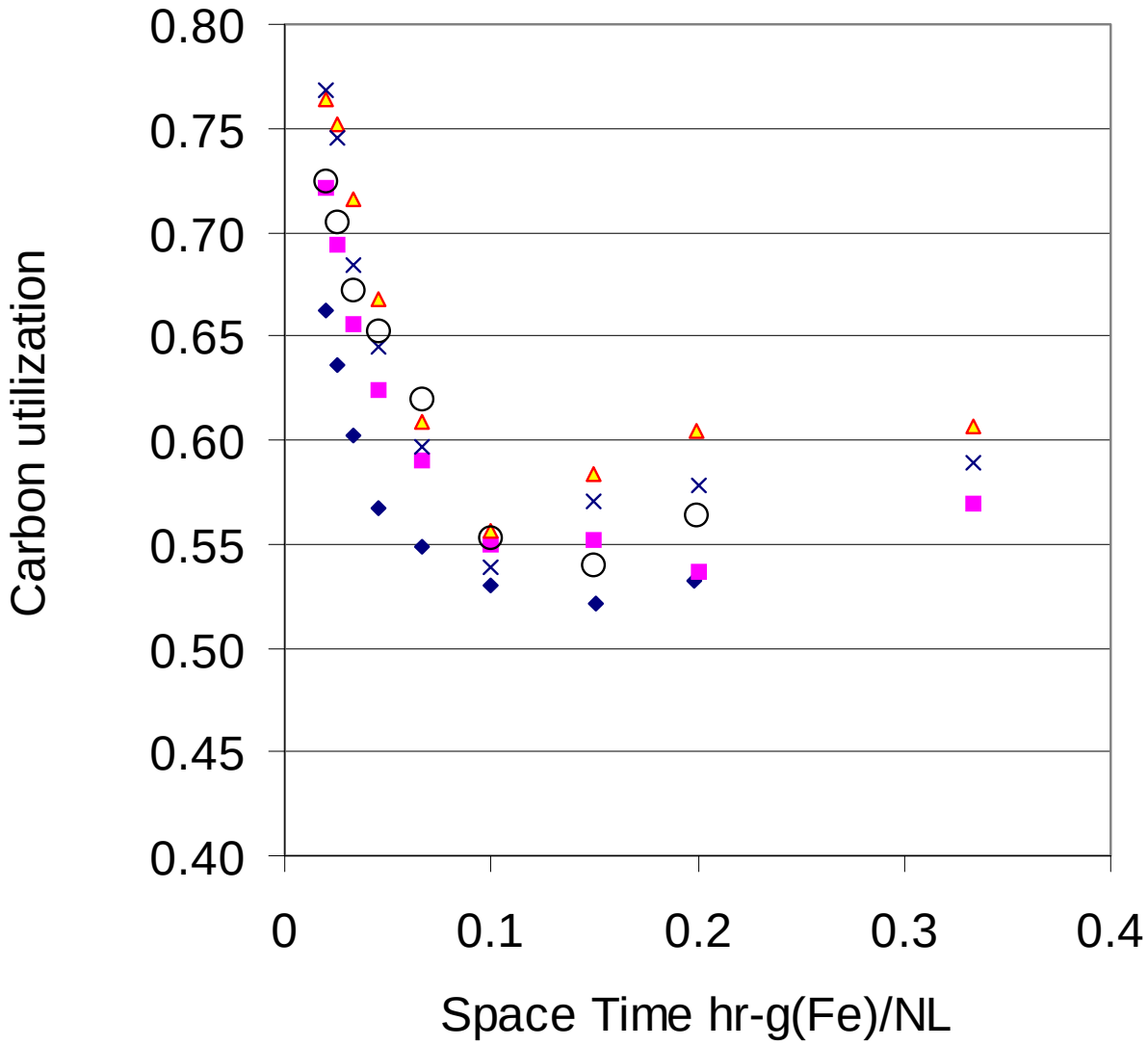

Figure 12. Effect of promoter on the carbon utilization (CO to hydrocarbon/CO converted) (◆, K; ■, Be; ▲, Mg; x, Ca; ", Ba).

Figure 13. Effect of promoter on alpha values

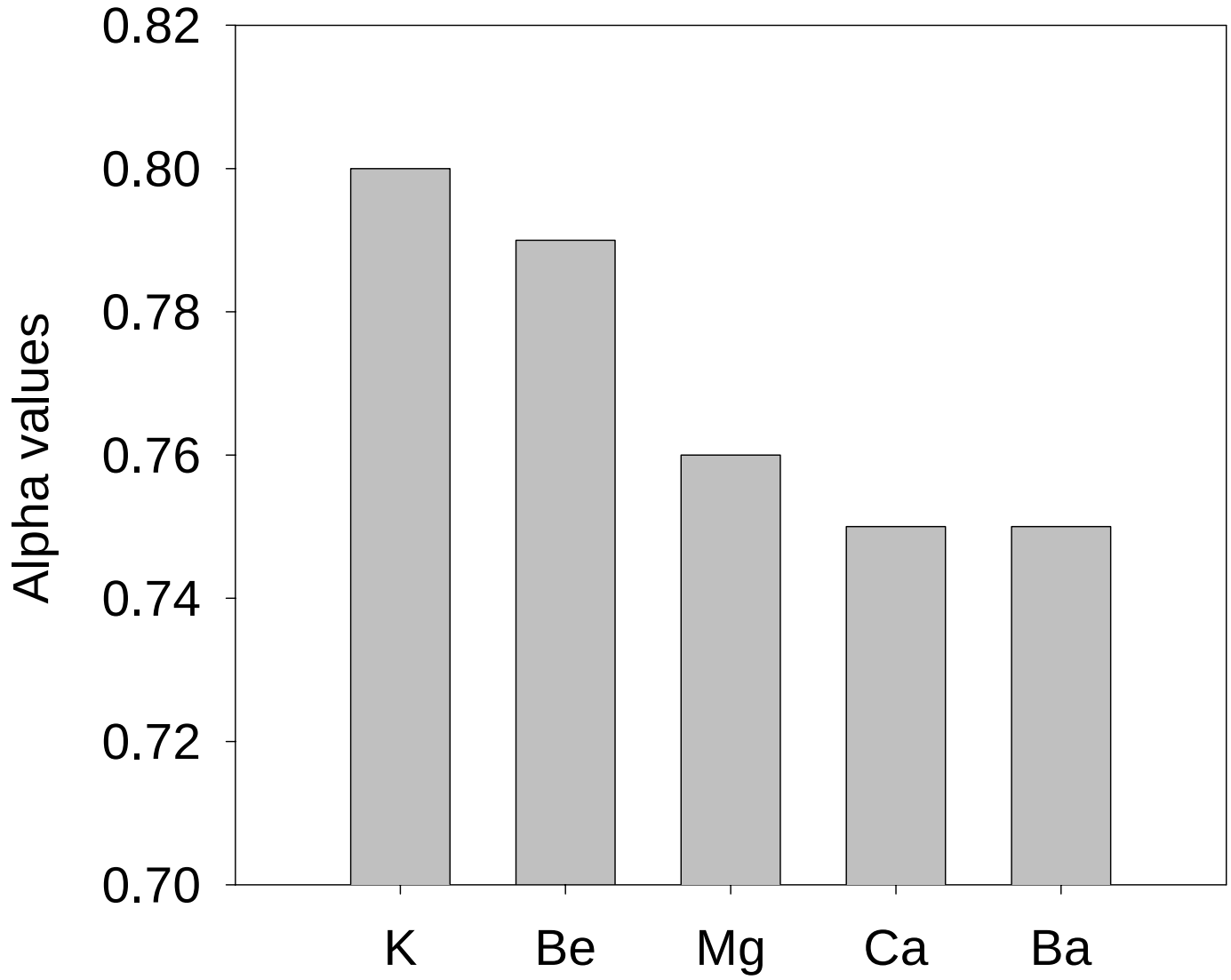

C. Effect of Structural Promoters on Iron Catalysts

Synthesis of the Catalysts

The Fe-Al samples were prepared by co-precipitation of iron and aluminum from nitrate solutions at constant pH of 8.5. Iron nitrate (1.3M) and aluminum nitrate (1.43M) solutions were mixed to yield a given Al/Fe ratio. Ammonium hydroxide (30%NH_3) was used as the precipitant. About 100 cm^3 deionized water was placed in a large beaker and heated to 85ºC using a magnetic stirrer/hotplate. The pH was adjusted to 8.5 by addition of an appropriate quantity of NH_4OH. The temperature was held at 85 ºC throughout the precipitation procedure. The solution of Fe^{3+} and Al^{3+} ions was added slowly to the beaker with continuous stirring. Simultaneously, the NH_4OH was added at a rate such that the pH was maintained at a constant value of 8.5. The resulting precipitate was filtered using vacuum filtration and washed with deionized water until the pH of the filtrate was measured to be in the range 7.0 to 7.5. The precipitate was subsequently dried in an oven overnight at 110ºC followed by calcination in static air at 400ºC for 10 hours. Samples were prepared that contained from 0% to ~25% Al. The samples were analyzed for iron content following calcination using ICP. The iron content by weight in the unpromoted samples was found to contain 70% Fe (average of 3 analyses) which agrees very well with the theoretical value of 69.994% in Fe_2O_3, confirming that the sample was hematite. XRD analysis also provided further proof that the samples contained hematite. Table 1 lists the compositions of the promoted iron catalysts.

The Fe-Si samples were already available in the lab. They were prepared by hydrolyzing an appropriate quantity of tetraorthosilicate (TEOS) in the acidic $Fe(NO_3)_3$ solution followed by precipitation using NH_4OH. They had silicon contents of up to ~8% Si, had been calcined at 400ºC and were used without any further treatment. Their compositions are summarized in Table 2.

XRD analysis of the samples showed that as the degree of loading of the promoter increased the samples became more amorphous. The samples were then treated in an oven at 600ºC for 24 hours to improve crystallinity.

BET Surface Area Measurements

Nitrogen sorption isotherms were measured using a Micromeritics TriStar 3000 instrument. Prior to analysis each sample was outgassed at 160ºC for at least 12 hours to a pressure less than 100 mTorr. The results of the analyses for the samples calcined at 400ºC and 600ºC are presented in Tables 3 and 4. It can readily be seen that as the quantity of the promoter is increased the surface area also increases. Also, as the temperature of the calcination is increased the surface area decreases. Representative plots illustrating the trend in change of surface area with increasing atomic percent of structural promoter for both the Al and Si additions are shown in Figures 1 and 2, respectively.

XRD Analysis

The samples containing varying atom percentages of the structural promoters Al or Si were prepared in order to investigate whether they are capable of entering into solid solution with the hematite and hence be well dispersed throughout the oxide mass. Whether or not these promoters had entered into solid solution was determined from their effect on the lattice parameters of the magnetite. Powder X-Ray Diffraction was used to determine the unit cell dimensions of the hematite. Hematite has a hexagonal structure and thus two cell dimensions, a_0 and c_0, had to be determined. X-Ray Diffractograms were obtained for all samples. Figures 3 and 4 show the diffractograms obtained for the Al and Si promoted iron oxide samples calcined at 400ºC. It can be seen that the Al promoted samples are not very crystalline at loadings greater than about 7 atom%. In contrast, the Si promoted samples are quite amorphous to X-Rays,

crystallinity only evident for the very small atomic fractions. It appears that the Si retards the crystallization of the Fe_2O_3 to a much greater degree than the presence of the Al. In order to make accurate lattice parameter determinations a greater degree of crystallinity is required so all the samples were heated in an oven to 600ºC for 24 hours and the resulting diffractograms are shown in Figures 5 and 6. In all cases Fe_2O_3 was identified as the only species present. At the higher levels of Al addition, 17.9% and 24.22%, there is evidence of another species present but this has yet to be identified. The ten most intense peaks of the diffractograms were each analyzed individually using the fitting program WINFIT to determine accurate peak locations in terms of 2θ. These 2θ values together with their corresponding Miller indices were input to the program UnitCell to calculate the lattice parameters for the hexagonal Fe_2O_3. It was found that as the quantity of the promoter increased there was a shift in all 2θ to higher values indicating that the promoter had entered the hematite lattice and was influencing its dimensions. These shifts in the lattice dimensions are shown as a function of the promoter concentration in Figures 7 to 10. The shift to higher 2θ values resulted in a decrease in both a_0 and c_0 lattice parameters. This is to be expected as the ionic radii of both Al^{3+} and Si^{4+}, 0.5Å and 0.41Å, respectively, are both less than that of Fe^{3+} (0.64Å), and would lead to a contraction of the unit cell. The shifts in the lattice dimensions are taken as evidence that the cations have entered into the hematite lattice.

Table 1

Al Content of the Samples

Sample	Al/Fe	Atom % Al
8A	---	0
10A	0.0118	1.17
3A	0.02	1.96
4A	0.044	4.21
5A	0.0706	6.6
6A	0.1335	11.77
7A	0.218	17.9
9A	0.3197	24.22

Table 2

Si Content of the Samples

Sample	Si/Fe	Atom % Si
FeSiO	---	0
$FeSi_2$	0.02	1.96
$FeSi_4$	0.044	4.21
$FeSi_8$	0.08	7.41

Table 3

Results of BET Analysis of Samples Treated at 400ºC

Sample	BET S.A. m^2/g	Pore Volume cm^3/g	Average Pore Radius nm
8A	33.44	0.19	11.4
10A	133.5	0.24	3.6
3A	46.19	0.2	8.5
4A	19.05	0.13	13.6
5A	99.6	0.25	4.9
6A	176.6	0.25	2.8
7A	232.6	0.24	2.1
9A	215.3	0.22	2.1
FeSiO	23.7	0.18	12.0
$FeSi_2$	78.9	0.2	5.1
$FeSi_4$	163.2	0.24	2.9
$FeSi_8$	193.5	0.24	2.5

Table 4

Results of BET Analysis of Samples Treated at 600ºC

Sample	BET S.A. m_2/g	Pore Volume cm^3/g	Average Pore Radius nm
8B	9.95	0.11	22.6
10B	11.6	0.12	20.9
3B	15.2	0.14	18.5
4B	14.9	0.11	14.4
5B	25.4	0.2	15.9
6B	36.4	0.22	11.9
7B	44.0	0.18	8.3
9B	52.9	0.18	6.6
FeSiOB	4.3	0.03	13.5
$FeSi_2B$	36.8	0.19	10.4
$FeSi_4B$	64.3	0.2	6.2
$FeSi_8B$	98.3	0.21	4.2

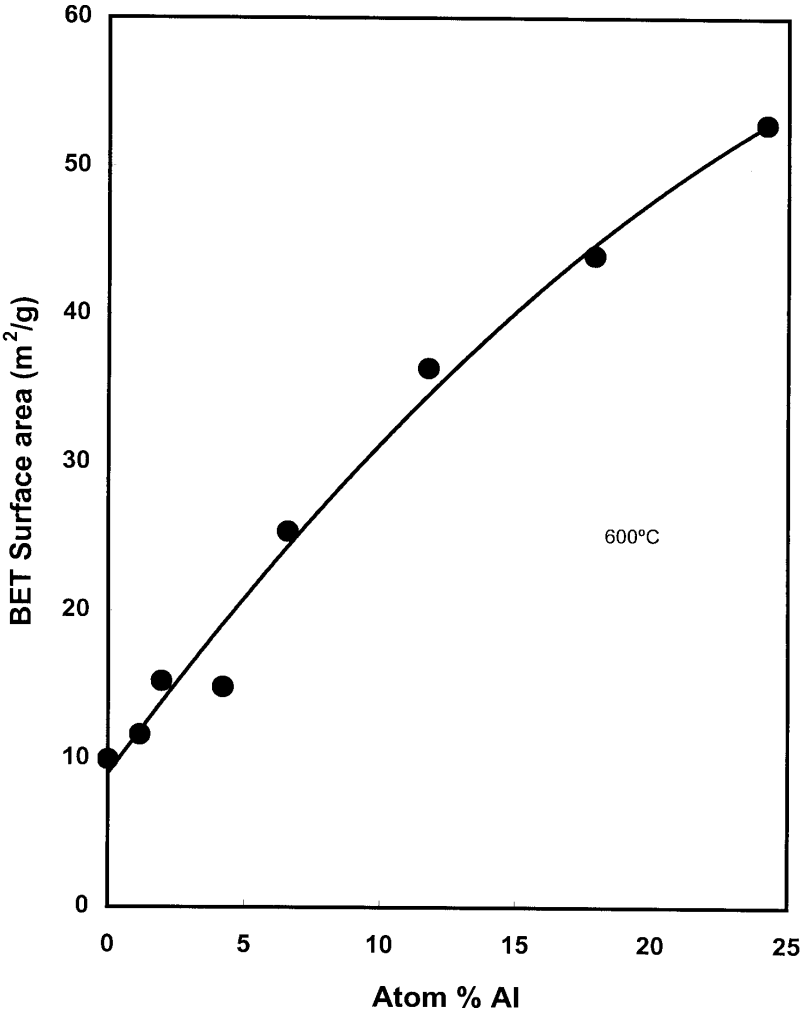

Figure 1. Variation of BET surface area with increasing atomc percent of Al. All samples were calcined at 600°C.

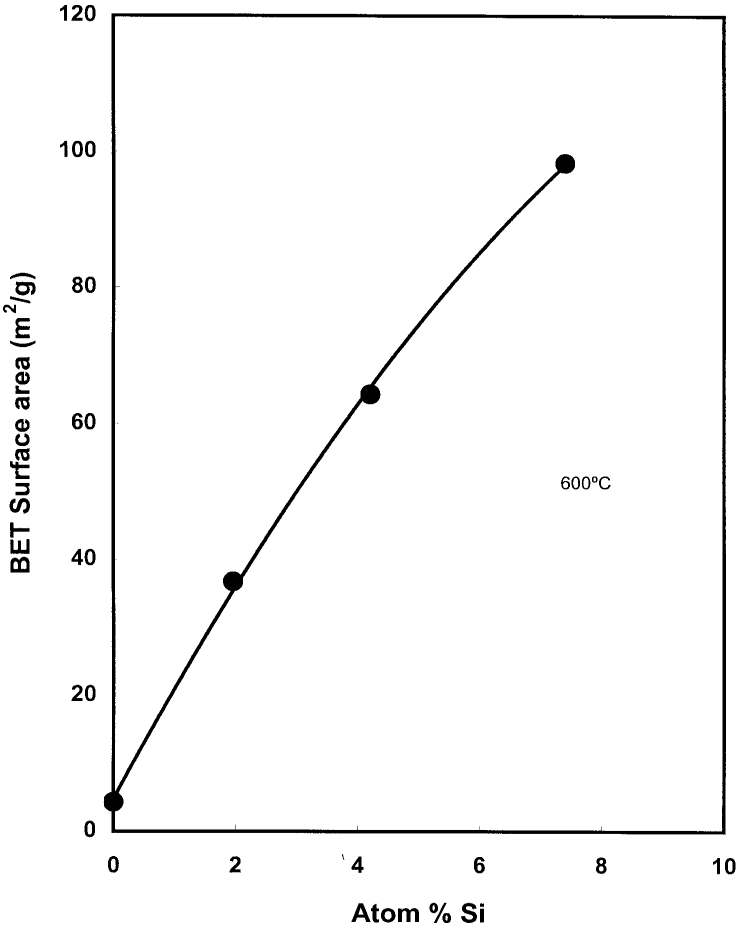

Figure 2. Variation of BET surface area with increasing atomic percent of Si. All samples were calcined at 600ºC.

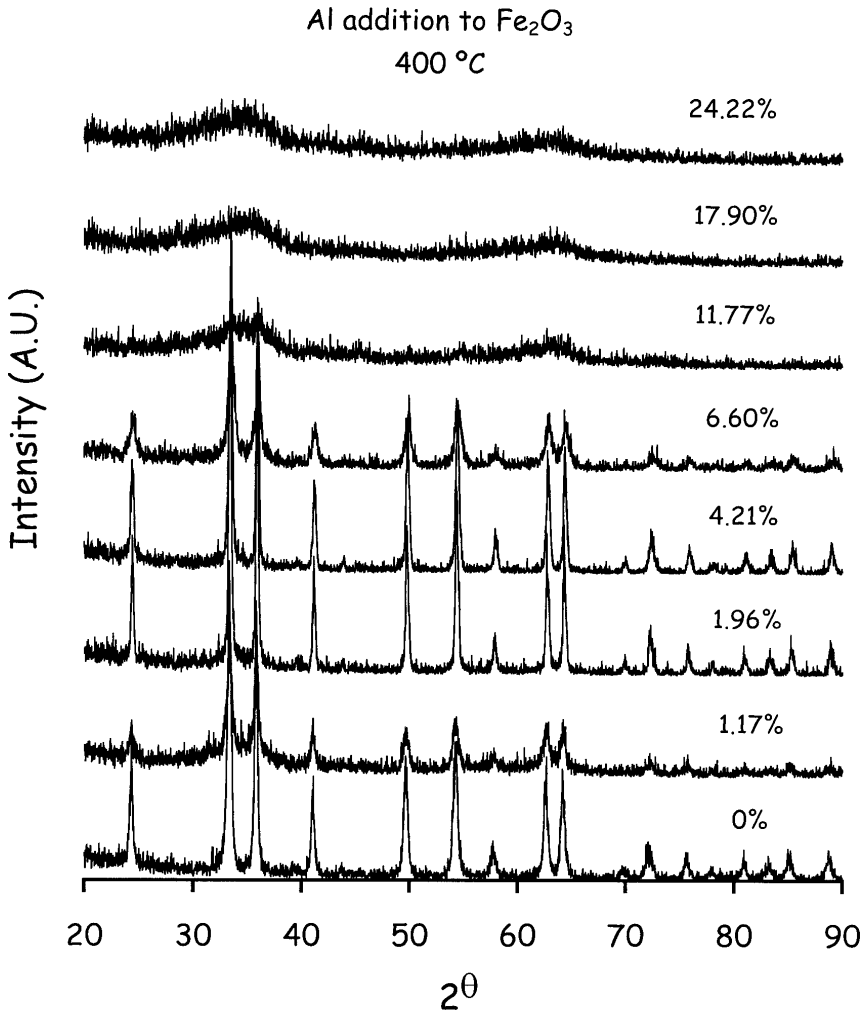

Figure 3. X-ray diffractograms of Al promoted hematite samples calcined at 400°C.

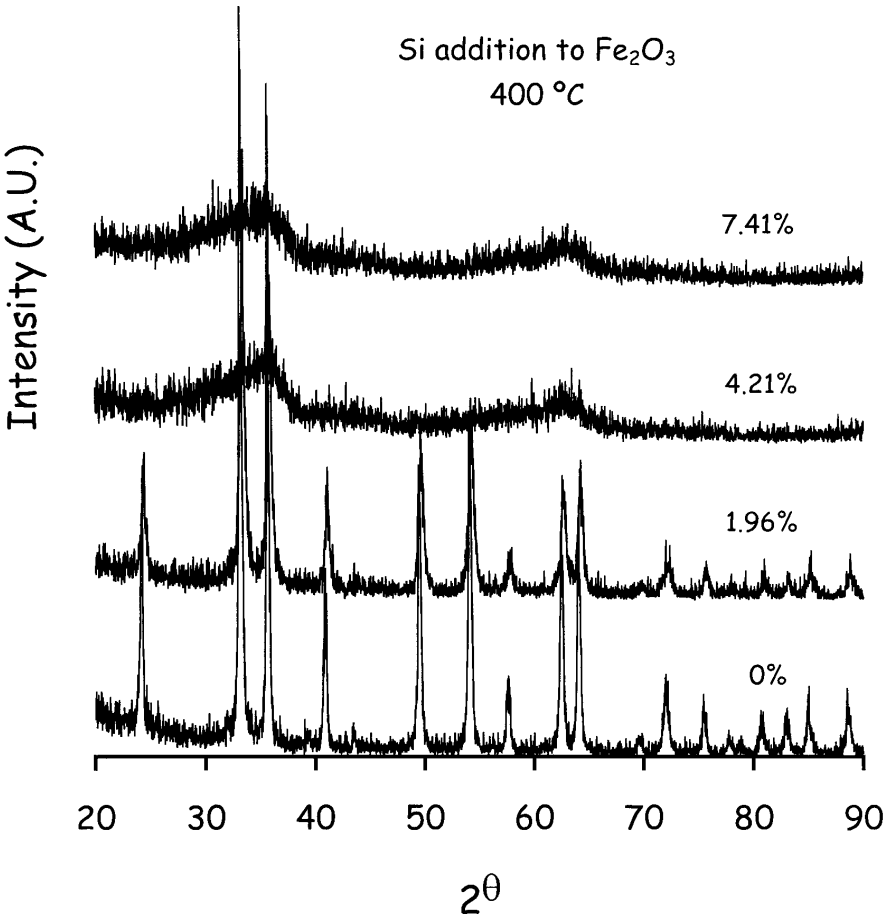

Figure 4. X-ray diffractograms of Si promoted hematite samples calcined at 400°C.

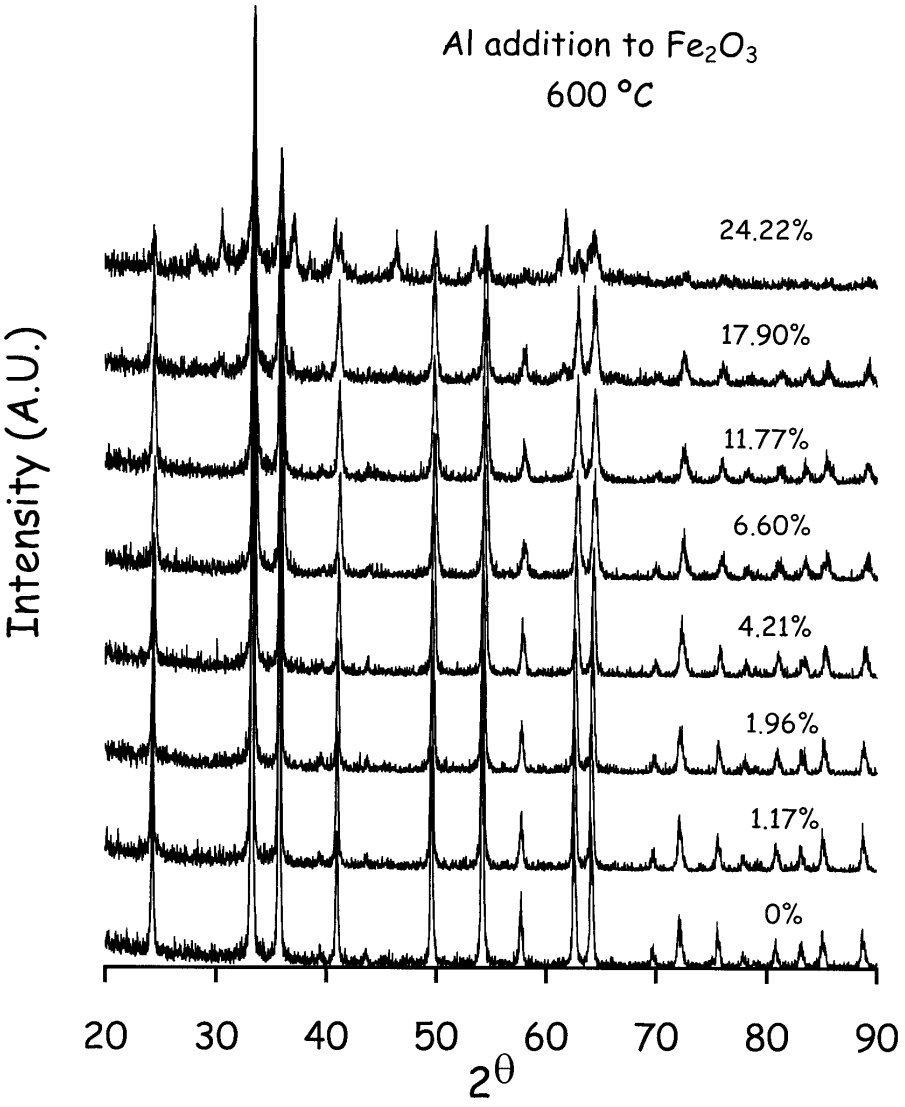

Figure 5. X-ray diffractograms of Al promoted hematite samples calcined at 600ºC.

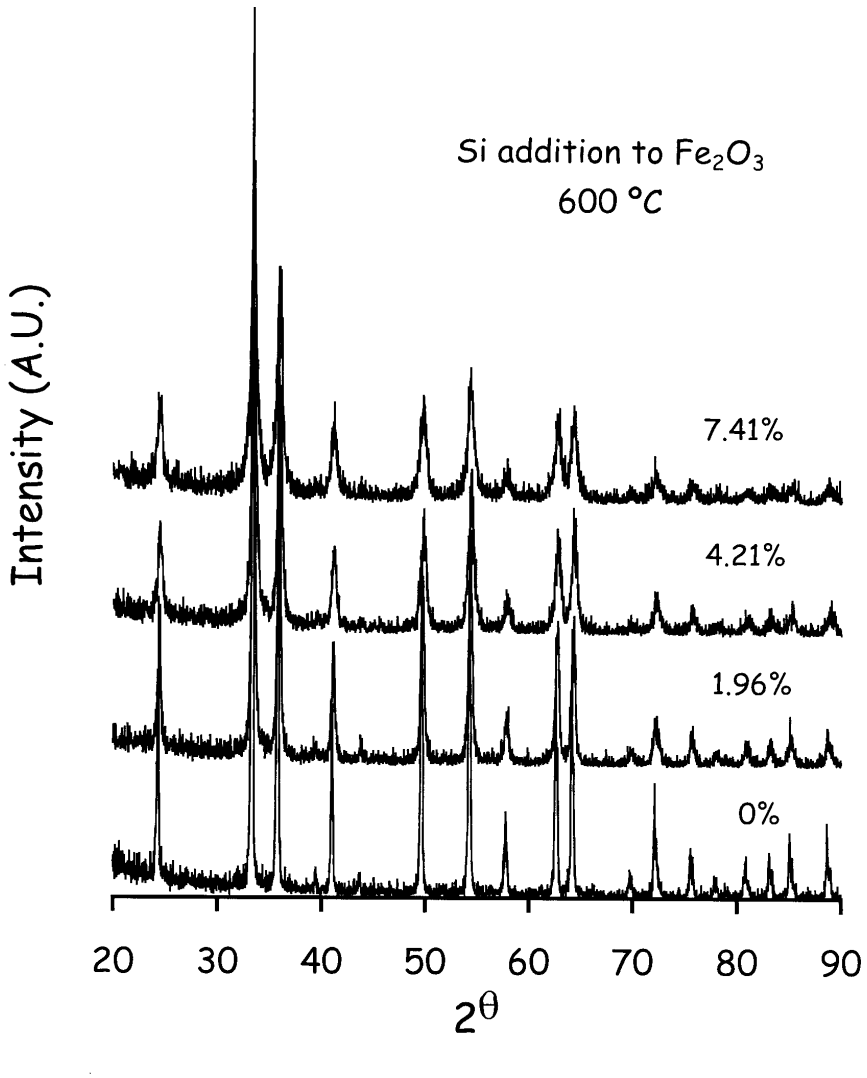

Figure 6. X-ray diffractograms of Si promoted hematite samples calcined at 600°C.

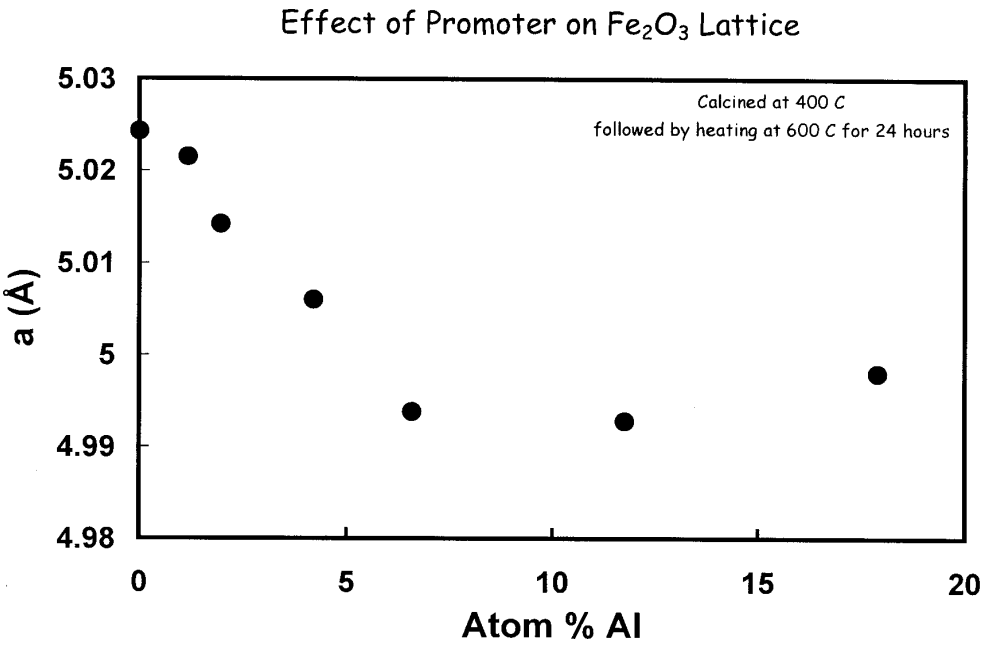

Figure 7. Variation of unit cell parameter a_0 with concentration of Al promoter.

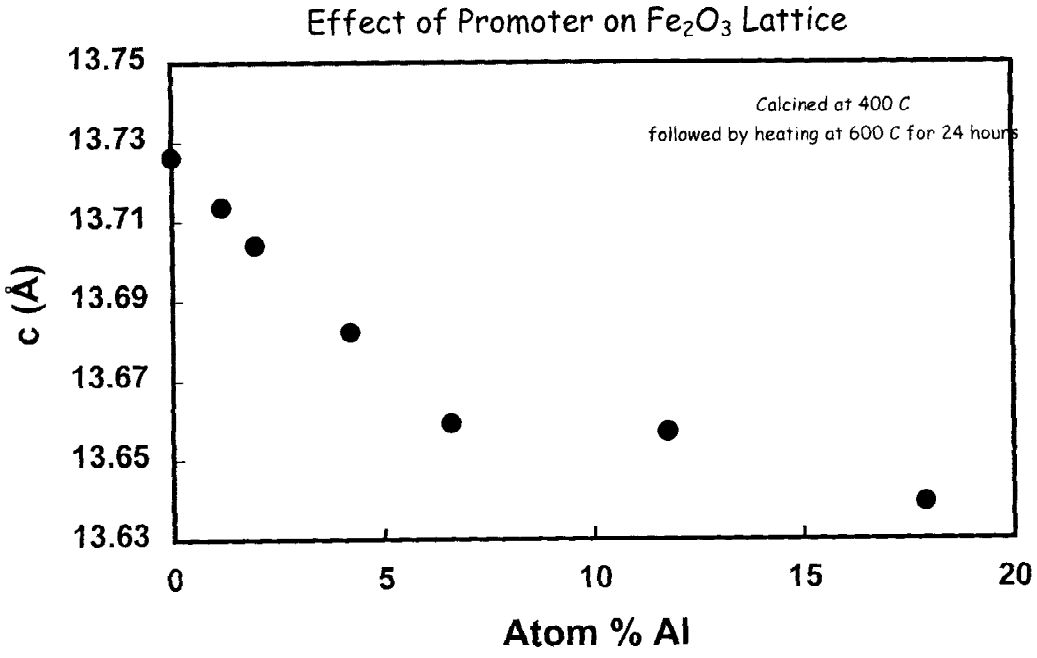

Figure 8. Variation of unit cell parameter c_0 with concentration of Al promoter.

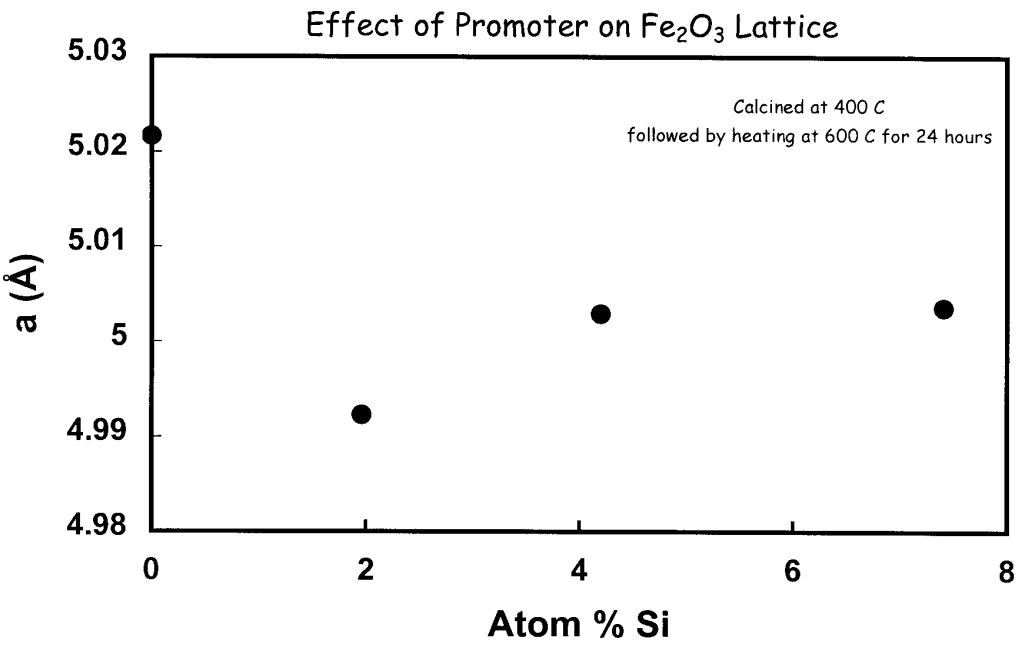

Figure 9. Variation of unit cell parameter a_0 with concentration of Si promoter.

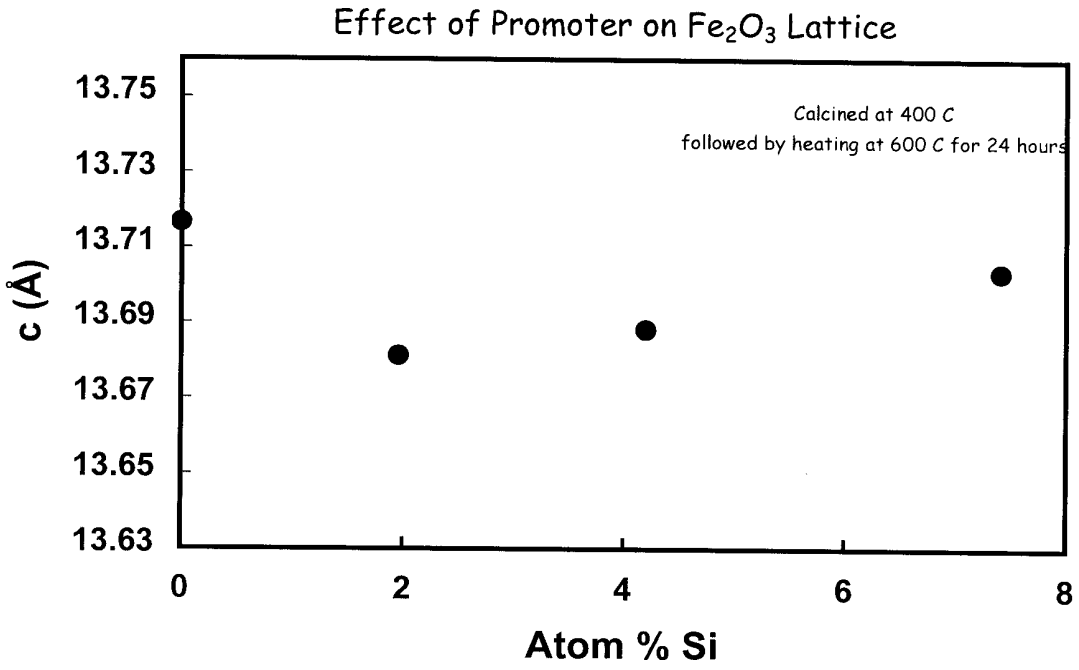

Figure 10. Variation of unit cell parameter c_0 with concentration of Si promoter.

D. Fischer-Tropsch Synthesis: Influence of Process Parameters on Activity and Selectivity of a Potassium Promoted Iron Catalyst

Abstract

Process parameters can play an important role in a chemical process. Study of the effect of reaction temperature, pressure and other parameters is necessary for process development, design and optimization. Factorial design is an effective approach for chemical process parametric studies. By experimental design, the number of trials was minimized. Although two-level factorial design failed to detect the nonlinearity of the process between the high- and low-level of factors concerned, it is still more effective to conduct several two-level experiments than to perform a series of three- to four-level experiments. Two-level factorial design can reveal both the single factor effect and the cross interactions between these factors. Results from this study show that temperature has the most important influence on CO and H_2 conversions, CO_2 and CH_4 selectivity and hydrocarbon production for this rate. Pressure and space velocity played a less significant role. Cross interactions between the factors are sometime not negligible, such as the interaction between temperature and other two factors (pressure and space velocity). Little difference in CO conversion was observed for FTS with 1.44 and 5.00 K:Fe catalysts at low temperature (230^{o}C). The two catalysts yielded similar CO_2 and CH_4 selectivity at a high temperature. Hydrocarbon rate was higher for K5.00 than the K1.44 catalyst.

Introduction

The Fischer-Tropsch synthesis (FTS) process, which converts carbon monoxide and hydrogen to hydrocarbons and oxygenates, makes coal or natural gas a promising alternative to petroleum. The mechanism and kinetics of the FTS process have been investigated (Dry, 1996; van der Laan and Beenackers, 1999; Raje and Davis, 1997; Adesina, 1996; Dry, 1981;

Zimmerman and Bukur, 1990; Ribeiro, et al., 1997; Hindermann, et al., 1993). The process can be simplified as the following two reactions:

$$nCO + (2n+1)H_2 \rightarrow C_nH_{2n+2} + nH_2O \ (FTS)$$

$$CO + H_2O \rightarrow CO_2 + H_2 \ (WGS)$$

Average molecular weight of the hydrocarbon products depends on reactions conditions and catalyst. When an iron catalyst is utilized in the FTS, a significant amount of carbon is consumed in the water gas shift (WGS) reaction, as shown by the second reaction. The complexity of the FTS process is the major obstacle in understanding the mechanism and defining the kinetics. A variety of proposals for the FTS mechanism are based on the surface species and various elementary reaction steps. Different kinetic equations were expressed in power-law based on the empirical data and the mechanism proposals from the literature (van der Laan and Beenackers, 1999).

Process parameters, i.e, reaction temperature, pressure and space velocity, have a significant influence on FTS kinetics, catalyst activity and selectivity. Due to the complexity of the FTS process, development of the FTS technology leads to the complications in the theoretical interpretation of the research data. A well designed experiment using statistic principles could sharply lower the cost of the experimental investigation. A common method to conduct the experiment is to change one factor at a time. Although it remains a conservative research approach, it is neither sufficient nor possible to detect the interactions between the factors involved. In this study, we investigate the effect of these process parameters, i.e., reaction temperature, pressure and space velocity, on carbon monoxide and hydrogen conversion, carbon dioxide and methane selectivity, and hydrocarbon rate. Experiments were conducted using a 3-factor, 2-level factorial design approach. The influence of each factor on

conversion and selectivity, and interactions between temperature, pressure and space velocity are discussed based on the experimental results.

Experimental

Preparation of Unpretreated Catalyst

Two iron catalysts promoted with potassium were prepared and tested in this study. Table 1 gives the compositions of the catalysts used in this study. The ratios shown in Table 1 are all atomic ratios relative to iron. Precipitated iron catalysts were prepared with tetraethyl orthosilicate, iron nitrate, potassium carbonate and copper nitrate.

Copper is widely used as a promoter for iron FTS catalyst. It was believed that copper can facilitate the activation process. Copper can also minimize the sintering of iron catalysts by lowering the reduction temperature (Dry, 1981). In this study, the 100Fe/4.6Si catalyst base powder was impregnated with the proper amount of aqueous $Cu(NO_3)_2 \bullet 3H_2O$ solution to give an atomic composition of 100Fe/4.6Si/2.0Cu. The amount of $Cu(NO_3)_2 \bullet 3H_2O$ added will depend on the iron content of the base catalyst. In addition to copper, potassium is also an important promoter for an iron catalyst to improve the FTS activity and selectivity. Details of catalyst preparation was given elsewhere (Luo and Davis, 2001).

In-situ Activation of Unpretreated Catalysts

The iron catalyst needs to be activated with H_2, CO or synthesis gas. Activation procedures can have a significant effect on the selectivity and activity of iron catalyst (Zimmerman and Bukur, 1990; Ribeiro, et al., 1997). It was reported that catalysts activated with CO yielded higher long-chain hydrocarbons than syngas and H_2 activated catalysts. In addition, activation conditions may also influence the activity and selectivity of the iron catalyst.

In this study, the potassium promoted iron catalysts were pretreated with CO at 270°C, 1.2 MPa for 24 hours. The reduction of Fe_2O_3 with CO occurs in two steps:

$$3Fe_2O_3 + CO \rightarrow 2Fe_3O_4 + CO_2$$

$$5Fe_3O_4 + 32CO \rightarrow 3Fe_5C_2 + 26CO_2$$

In addition, CO_2 and C may be formed by the Boudouard reaction:

$$2CO \rightarrow C + CO_2$$

Our previous work showed that approximately 50 % to 75% more carbon was present in the catalyst mass than was needed to form Fe_5C_2 (O'Brien, et al., 1996). Gradual oxidation of Fe_5C_2 to Fe_3O_4 was observed when iron catalyst was used in FTS and a catalyst with long-term stability consists of a mixture of Fe_3O_4 and iron carbides.

Reactor System

A one-liter continuous stirred tank reactor (CSTR) was used in this study. A sintered-metal filter was installed to remove the wax samples from the catalyst slurry. The wax sample was extracted through the internal filter and collected in the hot trap (200°C). A warm trap (100°C) and cold trap (0°C) were used to collect oil, light wax and water samples. Tail gas from the cold trap was analyzed with an HP quick GC.

A gas mixer fed with a CO and an H_2 stream fitted with mass controllers was used to provide a simulated synthesis gas with an H_2:CO ratio of 0.7. After the catalyst was activated with CO, syngas was introduced at a rate of 10 l-$hr^{-1}g^{-1}$ (based on iron). Reaction conditions were 230°C, 1.2MPa and a stirrer speed of 750 rpm.

Product Sampling and Analysis

Daily gas, water, oil, light and heavy wax samples were collected and analyzed. Table 2 gives the summary of the instruments for gas and liquid product analysis. A heavy wax sample was taken from the 200°C hot trap connected to the filter. Vapor phase above the slurry phase

passed to the warm (100°C) and the cold (0°C) traps outside the reactor. The light wax and water mixture was collected from the warm trap and an oil plus water sample from the cold trap. Tail gas from the cold trap was analyzed with an online HP Quad Series Micro GC. Molar compositions of C_1-C_7 olefins and paraffins were thus obtained. Hydrogen and carbon monoxide conversions were calculated based on the gas product GC analysis results and the gas flow measured at reactor outlet. Carbon monoxide conversion, CO_2 and CH_4 selectivity, and hydrocarbon rate were obtained using the following formulas:

$$CO\ Conversion = \frac{N_{CO-in} - N_{CO-out}}{N_{CO-in}} \bullet 100\%$$

$$CH_4\ Selectivity = \frac{N_{CH_4-out}}{(N_{CO-in} - N_{CO-out} - N_{CO_2-out})} \bullet 100\%$$

$$CO_2\ Selectivity = \frac{N_{CO_2-out}}{(N_{CO-in} - N_{CO-out})} \bullet 100\%$$

$$Hydrocarbon\ Rate = 14.3 \bullet \left(\frac{N_{CO-in} f}{M_{Iron}} - \frac{N_{CO_2-out}}{M_{Iron}} \right)$$

where N is the molar flow rate in moles/hour, f is the fractional conversion of CO, and M is the weight of active metal (Fe) in grams.

The oil and light wax samples were mixed before analysis with an HP 5790A GC. The heavy wax was analyzed with an HP5890 Series II Plus GC while the water sample was analyzed with an HP5890 GC.

Results and Discussions

Experiment Design

The purpose of factorial experimental design is to limit the number of experiments required to investigate the influence of the factors involved in a process. By proper design of the experiment, it is also possible to study the interaction between the factors concerned. In this study, FTS reaction temperature, pressure and space velocity were studied as the factors that affect the results of conversion and selectivity. A higher temperature may yielded a higher CO conversion, but it may also result in a higher undesired CO_2 and CH_4 selectivity. Studying the effect of each of these factors can lead to a better understanding of the process and establishment of a mathematical model that can be used in process design.

A process can be described by a mathematical expression as a function of factors x_1, x_2, x_3..., i.e.

$$Y = f(x_1+x_2+x_3+...)$$

This can be expressed with an approximate equation as follows:

$$Y = B_o + \sum_j B_j Z_j + \sum_{i<j} B_{ij} Z_i Z_j + \sum_j B_{jj} Z_j^{\,2} + \ldots$$

Two-level factorial experimental design can provide the maximum information from a minimum number of research trials (Anderson, 1974). It is believed that two-level factorial design is the most effective, although three- or four-level design can detect the nonlinearity in functional relationships between the factors and the response variable. However, two-level experiments require much fewer trials than a three- or four-level design so that it is more cost effective to conduct several two-level experiments than the latter.

An eight-run experiment was designed based on the three factor and two-level factorial design, as shown in table 3. It is important that the actual experiment was conducted in a

random order instead of the order listed in the table to ensure the integrity of the experiment. Based on literature and our own experience, a typical FTS conditions of 250°C, 2MPa and 7.5L $h^{-1}g$ was chosen as the middle point of the experimental variables. The low (-1) and high (+1) level pairs for temperature, pressure and space velocity were 230/270°C, 1.2/2.9 MPa and 5.0/10.0 SL $h^{-1}gFe^{-1}$, respectively. Figures 1 through 5 give the response of CO and H_2 conversion, hydrocarbon rate and CO_2 and CH_4 selectivity for the reaction catalyzed with a potassium ($g \cdot h^{-1}gFe^{-1}$) promoted iron catalysts.

The effect of a single factor is defined as the "main effect" and that between any two factors named as "interaction." While the main effect depicts the influence of a single factor, interaction effects describe the effect of one factor on the behavior of the other. Main effect is calculated by the following equation:

E_T = average response at low level of factor T- average response at high level of factor T

$$= \frac{(Y_{T2P1S1} + Y_{T2P1S2} + Y_{T2P2S1} + Y_{T2P2S2})}{4} - \frac{(Y_{T1P1S1} + Y_{T1P1S2} + Y_{T1P2S1} + Y_{T1P2S2})}{4}$$

where Y is the response such as CO conversion, CO_2 selectivity or hydrocarbon rate; T, P and S are three factors defined in this study, i.e., temperature, pressure and space velocity, respectively. A positive effect indicates the response variable changes in the same direction as the factor changes while a negative effect behaves the opposite.

Interaction effect between two factors is calculated in the same way:

I_{TP} = Effect of P at level 2 of Factor T - Effect of P at level 1 of Factor T

$$= \frac{(Y_{T2P2} - Y_{T2P1}) - (Y_{T1P2} - Y_{T1P1})}{2}$$

In case of a 3-factor experiment, interaction can also be calculated by substituting the four terms in the above equation as:

$$Y_{T2P2} = \frac{1}{2} \bullet (Y_{T2P1S1} + Y_{T2P1S2})$$
$$Y_{T2P1} = \frac{1}{2} \bullet (Y_{T2P1S1} + Y_{T2P1S2})$$
$$Y_{T1P2} = \frac{1}{2} \bullet (Y_{T1P2S1} + Y_{T1P2S2})$$
$$Y_{T1P1} = \frac{1}{2} \bullet (Y_{T2P1S1} + Y_{T2P1S2})$$

Carbon Monoxide and Hydrocarbon Conversion

Based on the above concepts, a factorial design and response scheme for each series of FTS reactions was designed as shown in Table 4. An eight-run experiment was carried out for each catalyst at two temperature, pressure and space velocity levels. The middle level of the variables was based of the literature and our previous work. Table 5 shows the results of two series of experiments using two potassium promoted iron catalysts. It is shown in Table 5 and Figure 1 that reaction temperature produced the largest effect on CO conversion when K1.44 (Fe:K = 100:1.44) catalyst was used. When temperature (Factor T) changed from 230 to 270^{o}C, average CO conversion increased by 26.8%. A much smaller effect of 6.64% was caused by pressure. Space velocity (Factor S) generated a negative effect on CO conversion because conversion decreased as the space velocity increased. Interactions between pressure and space velocity and the three-factor interaction are considered to be insignificant (<1%). Because of the normal experimental error, we neglect the two interaction effect (PS and TPS). The interaction between temperature and space velocity, and that between temperature and pressure were 5 and 8%, respectively. Reaction over K5.00 (Fe:K = 100:5) catalyst produced results (Table 5 and Figure 1) that are similar to the K1.44 catalyst. Temperature effect was as high as 31.08% and space velocity 20.70% while the effect of pressure and interactions of PS and TPS showed insignificant values (1-3%). Interaction between temperature and pressure was -8.78% and

between temperature and space velocity was -14.0% when K5.00 catalyst was used in FTS reaction.

Hydrogen conversion showed a behavior similar to CO conversion for FTS reaction over both potassium promoted iron catalysts. For both catalysts, temperature yielded an effect (25.0 and 26.9%) greater than that of space velocity (12.6 and 22.4%) on H_2 conversions. Pressure effect showed an even smaller effect on potassium promoted catalysts. All interaction effects were below 6%, which were much less important than a single main effect.

Figures 1 and 2 also show that the highest CO and H_2 conversions over potassium catalysts were obtained at high level of temperature and low level of space velocity. Pressure did not show an important role in CO and H_2 conversions as shown in Table 5 and Figures 1 and 2. Little change in CO conversion was observed between K1.44 and K5.00 catalyzed FTS reactions at low temperature (230^{o}C).

Methane Selectivity

Methane selectivity for potassium promoted catalysts was appreciably affected by temperature only. Neither pressure nor space velocity played an important role in methane selectivity. All interaction effects except that between temperature and pressure were insignificant. Average CH_4 selectivity at the low temperature level (230^{o}C) was 0.54 and 1.94% at 270^{o}C. A pressure increase from 1.2 to 2.9 MPa raised the CH_4 selectivity from 0.98 to 1.5% while an increase in space velocity showed little change in CH_4 selectivity. Interaction of temperature and pressure showed a value of -0.56% and the results in Table 5 revealed a negligible level of interactions between other factors. The FTS reaction over K5.00 catalyst showed similar results and showed a slightly lower effect of temperature and interaction between temperature and pressure. When temperature level changed from 230 to 270^{o}C, CH_4 selectivity increased from 0.96 to 1.85%, which is the largest main effect among all three factors. Similar

to K1.44 catalyst, K5.0 catalyst also revealed an interaction effect between temperature and pressure of 0.29%, which is the only appreciable value among all interactions. At a high temperature (270^{o}C), both K1.44 and K5.00 catalysts yielded similar methane selectivity as indicated in Figure 3.

Carbon Dioxide Selectivity

For both catalysts, temperature had a more important effect on CO_2 selectivity than pressure and space velocity. All interaction effects with the K1.44 catalyst were not appreciable while FTS over K5.00 catalyst showed a moderate interaction of 4.62 and -3.17% between TP and PS, respectively. As shown in Table 5, a temperature change from 230 to270^{o}C over K1.44 catalyst resulted in an average CO_2 selectivity increase by 19.3%. When the K5.0 catalyst was utilized, a temperature increase resulted in a CO_2 increase by 16.2%. Pressure effect over potassium promoted catalysts, however, showed a much less important effect than that of temperature. Carbon dioxide selectivity decreased by 1.59% over K1.44 catalyst and by 7.18% over K5.00 catalyst when pressure changed from 1.2 to 2.9 MPa. Similarly, CO_2 selectivity decreased by 5.48% over K1.44 catalyst and by 5.74% over K5.00 catalyst were found when the space velocity increase from 5.0 to 10.0 $SLh^{-1}gFe^{-1}$.

Hydrocarbon Rate

Similar to all other effects, temperature had the most important influence on hydrocarbon rate. As shown in Table 5, a temperature change from 230 to 270^{o}C resulted in an increase in hydrocarbon rate by 0.41 g/h/g-Fe over K1.44 catalyst and by 0.34 g/h/g-Fe over K 5.00 catalyst. Pressure and space velocity, however, affected the hydrocarbon rate to a much less extent, ranging from 0.04 to 0.14 g/h/g-Fe when potassium promoted catalysts were utilized. It is also found from Table 5 that the effect of pressure was greater than that of space velocity when K1.44 catalyst was used while the opposite result was observed when the K 5.00 catalyst was used. All

interaction effects were insignificant when K1.44 potassium promoted catalysts were used. When K5.00 catalyst was used, interactions between TS and TPS were -0.20 and -0.12, respectively. The other two interactions (TS and PS) were only 0.06 and -0.07.

Figure 5 shows that overall hydrocarbon rate over K5.00 catalyst is significantly higher than over K1.44 catalyst. As shown in Figure 5, a hydrocarbon rate of 0.68 $gh^{-1}gFe^{-1}$ was obtained when K.500 catalyst was used while the K1.44 catalyst yielded only 0.17 $gh^{-1}gFe^{-1}$ hydrocarbon under the same condition. When K5.00 catalyst was used, hydrocarbon yields at the first six data points were two to three times higher than that when K1.44 catalyst was used.

Conclusions

Factorial design is an effective approach for studying process parameters. By designing the experiment, the number of trials was minimized and the cost and time were significantly saved. Although two-level factorial design failed to detect the nonlinearity of the process between the high and low level of factors concerned, it is still the more effective way to conduct several two-level experiments than to perform a series of experiment of three- or four-level. In addition, two-level factorial design reveals the interactions between factors.

Acknowledgment

This work was supported by U.S. DOE contract number DE-FC26-98FT40308 and the Commonwealth of Kentucky.

Nomenclature

Y	Response
E	Main effect of a factor
I	Interaction between factors
N	Molar flow (mol/hr)
f	Fractional conversion (%)

Subscript

T	Reaction temperature
P	Reaction pressure
S	Space velocity
T1	Temperature at low level
T2	Temperature at high level
P1	Pressure at low level
P2	Pressure at high level
S1	Space velocity at lower level
S2	Space velocity at high level

References

Adesina, A. A., Appl. Catal. A 138 (1996).

Anderson, V. L., Design of Experiments II, Marcel Dekker, Inc., New York (1974).

Dry, M. E., in: J.R. Anderson, M. Boudart (Eds.), *Catalysis-Science and Technology*, Vol. 1, Springer, New York (1981).

Dry, M.E., *Appl. Catal.* A 138 (1996).

Hindermann, J. P., Hutchings, G. J., Kiennemann, A., *Catal. Rev.-Sci. Eng.* 35 (1993).

Lochner, R. H., in *Quality planning, control, and improvement in research and development*, edited by George W. Roberts, Marcel Dekker, Inc, New York (1994).

Luo, M., Davis, B. H., *Stud. in Surf. Sci. and Catalysis*, Proceedings of the 9th International Symposium on Catalyst Deactivation, Vol. 139, 133 (2001).

O'Brien, R. J., Xu, L., Spicer, R. L., Davis, B. H., Energy & Fuels, 10, 921 (1996).

Raje, A. P., Davis, B. H., Catalysis Today, Volume 36, Issue 3, 6 June 1997.

Ribeiro, F. H., Schach von Wittenau, A. E., Bartholomew, C. H., Somorjai, G. A., *Catal. Rev.-Sci. Eng*. 39 (1997).

Van der Laan, G. P., Beenackers, A. A. C. M., *Catal. Rev.-Sci. Eng*. 41, 255 (1999).

Zimmerman, W. H., Bukur., D. B., *Can. J. Chem. Eng*. 68, 292 (1990).

Table 1

Alkali Promoted Catalysts used in this Study[a]

Catalyst ID	Fe	Si	Cu	K	Catalyst Loading (g) [b]
K 1.44	100	4.6	2.0	1.44	9.59
K 5.00	100	4.6	2.0	5.00	32.20

a. Atomic ratio.
b. Grams catalyst in 300g start-up oil.

Table 2 Analyzers for FTS Products		
Analyzer	Sample	GC Detector
HP Quad Series Micro GC	Gas	TCD
HP 5890 GC Series II	Water	TCD
HP 5790A GC	Oil + Light Wax	FID
HP 5890 Series II Plus	Heavy Wax	FID

Table 3

Three-Factor and Two-Level Factorial Experiment Plan

Run ID	Temperature (^{o}C)	Pressure[a] (MPa)	Space Velocity (SL h^{-1}g-Fe^{-1})
A	230	1.2	5
B	230	1.2	10
C	230	2.9	5
D	230	2.9	10
E	270	1.2	5
F	270	1.2	10
G	270	2.9	5
H	270	2.9	10

a. Gauge pressure.

Table 4

Experiment Design and Response Scheme for CO Conversion Study with K1.44 Catalyst

Standard Run Order	Actual Run Order	Response (CO Conversion)	Temperature		Pressure[a]		Space Velocity	
			Factor T		Factor P		Factor S	
			Level	(°C)	Level	(MPa)	Level	(SL h^{-1} gFe^{-1})
A	3	21.6	-1	230	-1	1.2	-1	5
B	8	15.9	-1	230	-1	1.2	+1	10
C	1	22.1	-1	230	+1	2.9	-1	5
D	6	17.3	-1	230	+1	2.9	+1	10
E	5	49.4	+1	270	-1	1.2	-1	5
F	7	30.3	+1	270	-1	1.2	+1	10
G	4	63.2	+1	270	+1	2.9	-1	5
H	2	21.1	+1	270	+1	2.9	+1	10

a. Gauge pressure.

Table 5

Summary of Effect Analysis from Three-Factor Two-Level Experiment Design

Response Variable	Catalyst ID	Average Response	Factor T (^oC)	Factor P (MPa)	Factor S ($Sl\ h^{-1}gFe^{-1}$)	Interaction TP	Interaction TS	Interaction PS	Interaction TPS
CO Conversion (%)	K1.44	32.6	26.8	6.64	-13.0	5.69	-7.67	-0.51	-1.00
	K5.00	34.5	31.1	-2.38	-20.7	-8.78	-14.0	1.61	-3.07
H_2 Conversion (%)	K1.44	30.1	26.9	10.7	-12.6	4.83	-5.66	-1.83	1.22
	K5.00	34.8	25.0	1.48	-22.4	-4.26	-6.15	-2.05	1.70
CH_4 Selectivity (%)	K1.44	1.24	1.39	0.52	0.01	-0.56	0.05	-0.08	-0.03
	K5.00	1.40	0.89	0.07	-0.04	0.29	-0.02	-0.11	0.01
CO_2 Selectivity (%)	K1.44	28.9	19.3	-1.59	-5.48	0.60	-0.53	-0.18	-1.26
	K5.00	35.2	16.2	-7.18	-5.74	4.62	0.44	-3.17	0.43
Hydrocarbon Rate ($g\ h^{-1}gFe^{-1}$)	K1.44	0.34	0.41	0.14	0.06	0.08	0.04	0.03	0.04
	K5.00	0.55	0.34	0.04	0.11	-0.20	-0.07	0.06	-0.12

Figure 1. CO Conversion

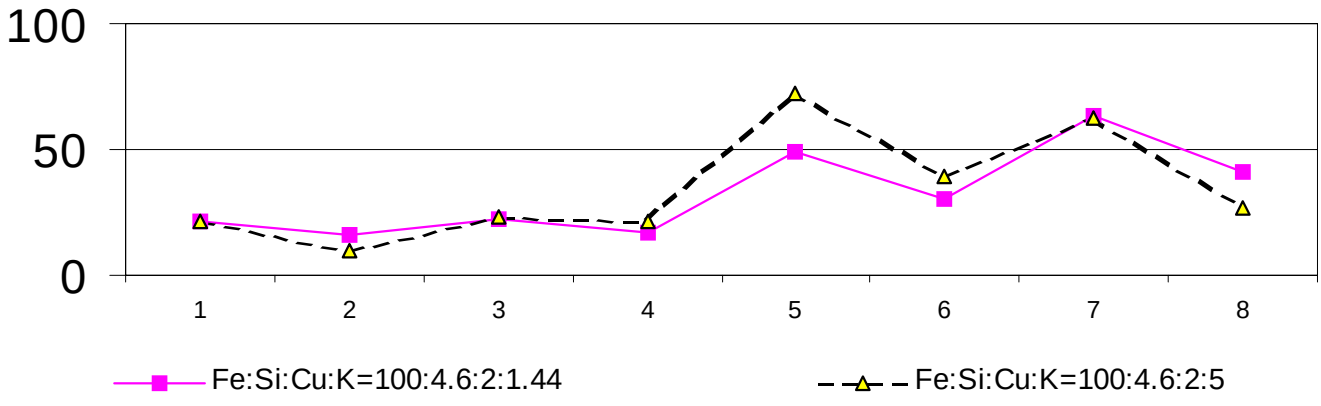

1: 230°C, 2.9MPa, 5 SL $h^{-1}gFe^{-1}$; 2: 230°C, 2.9MPa, 10 SL $h^{-1}gFe^{-1}$;
3: 230°C, 1.2MPa, 5 SL $h^{-1}gFe^{-1}$; 4: 230°C, 1.2MPa, 10 SL $h^{-1}gFe^{-1}$;
5: 270°C, 2.9MPa, 5 SL $h^{-1}gFe^{-1}$; 6: 270°C, 2.9MPa, 10 SL $h^{-1}gFe^{-1}$;
7: 270°C, 1.2MPa, 5 SL $h^{-1}gFe^{-1}$; 8: 270°C, 1.2MPa, 10 SL $h^{-1}gFe^{-1}$

Figure 2. H_2 Conversion

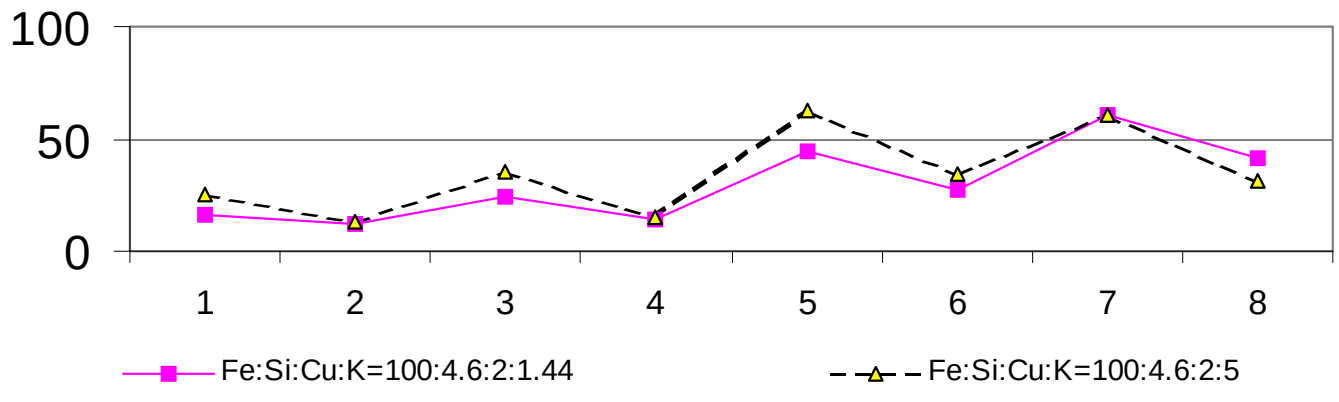

1: 230°C, 2.9MPa, 5 SL $h^{-1}gFe^{-1}$; 2: 230°C, 2.9MPa, 10 SL $h^{-1}gFe^{-1}$;
3: 230°C, 1.2MPa, 5 SL $h^{-1}gFe^{-1}$; 4: 230°C, 1.2MPa, 10 SL $h^{-1}gFe^{-1}$;
5: 270°C, 2.9MPa, 5 SL $h^{-1}gFe^{-1}$; 6: 270°C, 2.9MPa, 10 SL $h^{-1}gFe^{-1}$;
7: 270°C, 1.2MPa, 5 SL $h^{-1}gFe^{-1}$; 8: 270°C, 1.2MPa, 10 SL $h^{-1}gFe^{-1}$

Figure 3. Methane selectivity

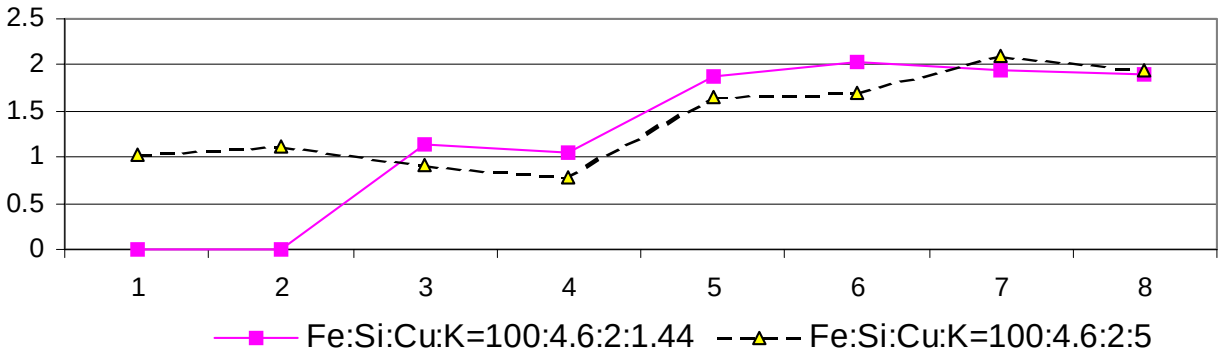

1: 230°C, 2.9MPa, 5 SL $h^{-1}gFe^{-1}$; 2: 230°C, 2.9MPa, 10 SL $h^{-1}gFe^{-1}$;
3: 230°C, 1.2MPa, 5 SL $h^{-1}gFe^{-1}$; 4: 230°C, 1.2MPa, 10 SL $h^{-1}gFe^{-1}$;
5: 270°C, 2.9MPa, 5 SL $h^{-1}gFe^{-1}$; 6: 270°C, 2.9MPa, 10 SL $h^{-1}gFe^{-1}$;
7: 270°C, 1.2MPa, 5 SL $h^{-1}gFe^{-1}$; 8: 270°C, 1.2MPa, 10 SL $h^{-1}gFe^{-1}$

Figure 4. CO_2 Selectivity

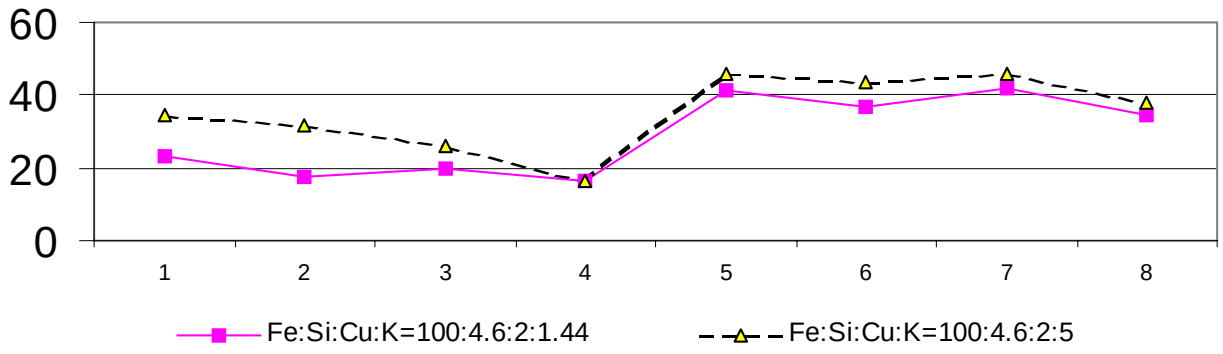

1: 230°C, 2.9MPa, 5 SL $h^{-1}gFe^{-1}$; 2: 230°C, 2.9MPa, 10 SL $h^{-1}gFe^{-1}$;
3: 230°C, 1.2MPa, 5 SL $h^{-1}gFe^{-1}$; 4: 230°C, 1.2MPa, 10 SL $h^{-1}gFe^{-1}$;
5: 270°C, 2.9MPa, 5 SL $h^{-1}gFe^{-1}$; 6: 270°C, 2.9MPa, 10 SL $h^{-1}gFe^{-1}$;
7: 270°C, 1.2MPa, 5 SL $h^{-1}gFe^{-1}$; 8: 270°C, 1.2MPa, 10 SL $h^{-1}gFe^{-1}$

Figure 5. Hydrocarbon rate

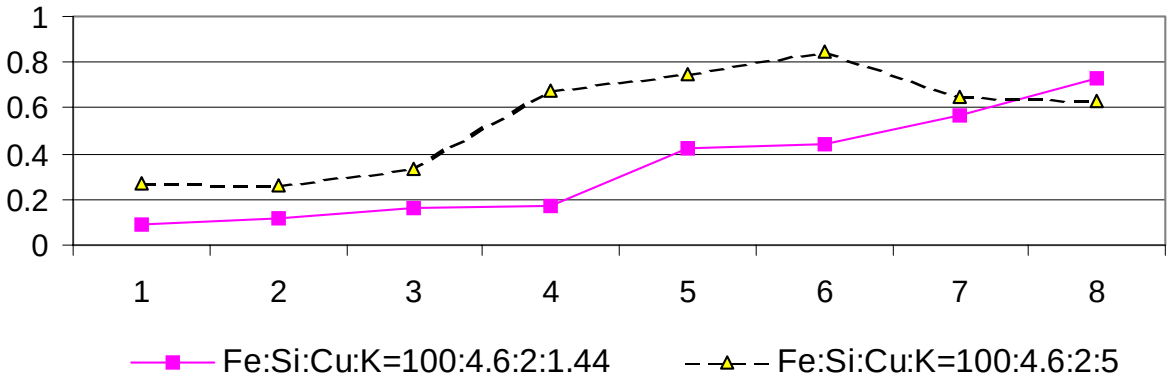

1: 230°C, 2.9MPa, 5 SL $h^{-1}gFe^{-1}$; 2: 230°C, 2.9MPa, 10 SL $h^{-1}gFe^{-1}$;
3: 230°C, 1.2MPa, 5 SL $h^{-1}gFe^{-1}$; 4: 230°C, 1.2MPa, 10 SL $h^{-1}gFe^{-1}$;
5: 270°C, 2.9MPa, 5 SL $h^{-1}gFe^{-1}$; 6: 270°C, 2.9MPa, 10 SL $h^{-1}gFe^{-1}$;
7: 270°C, 1.2MPa, 5 SL $h^{-1}gFe^{-1}$; 8: 270°C, 1.2MPa, 10 SL $h^{-1}gFe^{-1}$